

POLITECNICO DI TORINO

Master of Science in Mechatronic Engineering

Master Degree Thesis

**A robust control approach to the  
problem of the sea wave energy  
conversion**



**Supervisors**

prof. Regruto Tomalino Diego  
prof. Canale Massimo  
prof. Cerone Vito

**Candidate**

Cosimo Schifone

ACADEMIC YEAR 2019-20



# Acknowledgements

The last moments of the academic years are ending, the university life is reaching the terminal stop. The past years have represented probably the most formative in my life, not only to an academic point of view, but especially to life one. It is now my duty to pass to the important step of the acknowledgements.

Firstly I want to thanks my professor Diego Regruto and all the SIC group for the big opportunity given to me, for aid and instruction allowed in each moment.

The most important thanks and all my gratitude goes to my parents, which have constituted my strong rock in every moment and in each decision. It is due to their teaching and sacrifices that I am here, in this point.

Thanks to Marianna, that has given to me the right charge in some moments where no adults and no friends words were correct and encouraging but only a sister words could be right, and thanks to Claudio and Alessandro which cover an important part in my life.

It is a duty to thanks my grandparents, my uncles and all the big family that always supported me.

I would like to thanks also my friends, my real friends, which have shared with me errors, quarrels, fun and growing up.

Finally, I want to thanks Roberta, which has been present in every moment of the master degree years, which has spent her effort also for me and has given smiles, force and courage in most difficult moments.

Thanks to all of you, this important goal is not only mine, it wouldn't have been possible without you.

# Summary

The thesis project is oriented to the Inertial Sea Wave Energy Converter (ISWEC). The ISWEC is an electrical system that converts the incident wave power into electrical energy, developed by the DIMEAS Department at Politecnico di Torino (G.Bracco, E.Giorcelli, G.Mattiazzo). The basic work principle is to use the gyroscopic effect in order to take in motion a shaft connected to a PTO unit(Power Take Off), so damping such rotation with a proper torque the electrical energy is obtained. The main goal is to find a controller through the Robust Control approach with H-inf techniques, based on reference tracking error, such that the produced power is comparable to the previous MPC controller, that presents optimal conversion energy but high computational requirements. In order to find a plant that can approximate the real one, the Set-Membership approach is used, with a set of input-output data available from a Simulink scheme of MPC case study. In the work different cases are proposed to show the main results and the limits of this approach.

# Contents

<b>List of Figures</b>	6
Motivation . . . . .	8
Thesis organization . . . . .	8
<b>1 Iswec system</b>	9
Introduction . . . . .	9
Linear model . . . . .	11
<b>2 Set membership identification</b>	13
2.1 Basic notions . . . . .	13
2.1.1 Error representation . . . . .	13
2.1.2 Feasible Parameter Set and Polynomial optimization problem	15
2.1.3 SparsePOP tool . . . . .	18
2.2 Set-membership in ISWEC model . . . . .	19
2.2.1 Model requirements . . . . .	19
2.2.2 Low order model identification . . . . .	22
2.2.3 High order model identification . . . . .	30
<b>3 Robust Control</b>	35
3.1 Basic notions . . . . .	35
3.1.1 Model uncertainty . . . . .	39
3.1.2 Robust control through $H_\infty$ . . . . .	41
3.2 Robust Control in ISWEC model . . . . .	44
3.2.1 Low order model $H_\infty$ approach . . . . .	44
3.2.2 High order model $H_\infty$ approach . . . . .	51
<b>4 Non linear validation</b>	57
<b>5 Conclusions</b>	65
<b>Bibliography</b>	67

# List of Figures

1.1	ISWEC layout . . . . .	9
2.1	Eq.error structure . . . . .	14
2.2	Errors in variables structure . . . . .	14
2.3	Output error structure . . . . .	14
2.4	Parameter uncertainty interval . . . . .	16
2.5	Convex relaxation scheme . . . . .	17
2.6	Convex hull . . . . .	18
2.7	Iswec MPC . . . . .	20
2.8	Model structure . . . . .	21
2.9	Wave 3 tracking result . . . . .	26
2.10	Wave 3 optimal tracking result . . . . .	26
2.11	Wave 4 tracking result . . . . .	27
2.12	Wave 4 optimal tracking result . . . . .	27
2.13	Wave 7 tracking result . . . . .	28
2.14	Wave 7 optimal tracking result . . . . .	28
2.15	Wave 9 tracking result . . . . .	29
2.16	Wave 9 optimal tracking result . . . . .	29
3.1	Feedback system . . . . .	35
3.2	Bode diagram . . . . .	36
3.3	Disturbance constraints . . . . .	38
3.4	Multiplicative uncertainty model . . . . .	40
3.5	Conservative uncertainty model . . . . .	41
3.6	Generalized plant model . . . . .	42
3.7	Total generalized plant model . . . . .	43
3.8	$H_\infty$ feedback system . . . . .	44
3.9	$H_\infty$ Feedback block schemes . . . . .	44
3.10	Bode diagram of $W_T$ and $W_u$ . . . . .	47
3.11	Tracking of the reference with low order controller . . . . .	48
3.12	Tracking error of the reference with low order controller . . . . .	48
3.13	Torque with low order controller . . . . .	49
3.14	Power with low order controller . . . . .	49
3.15	Robust stability condition with low order controller . . . . .	50
3.16	Nominal performance condition with low order controller . . . . .	50

3.17	Robust performance condition with low order controller . . . . .	51
3.18	Bode diagram of $W_T$ and $W_u$ . . . . .	52
3.19	Tracking of the reference with high order controller(case 1) . . . . .	53
3.20	Torque with high order controller(case 1) . . . . .	53
3.21	Power with high order controlle(case 1) . . . . .	54
3.22	Tracking of the reference with high order controller(case 2) . . . . .	55
3.23	Torque with high order controller(case 2) . . . . .	55
3.24	Power with high order controller (case 2) . . . . .	56
4.1	Non linear Simulink model . . . . .	57
4.2	Non linear simulation output . . . . .	58
4.3	Non linear simulation torque . . . . .	58
4.4	Original model . . . . .	59
4.5	New concept model . . . . .	59
4.6	Tracking for wave3 . . . . .	62
4.7	Produced power for wave3 . . . . .	62

## Motivation

From the 1997, through the White Paper on renewable energy sources (RES), the Europe started radically to introduce the concept of RES, marking an international and global need of new consumption roads ([2]). In December 2018, the next important step was taken under the Paris Agreement, in order to make Europe a global leader in renewables. The usage of biofuel and biogas for transport sector, the decarbonisation in industries, are only few of the required, and necessary, requisites of this new approach. The ocean energy guarantees an optimal resource, in terms of security of supply and reduction of  $CO_2$  emissions, and is becoming an important interested target in many countries, in terms of tidal energy, ocean thermal energy, and especially wave energy ([1]). The system taken in analysis in the thesis work is the Inertial Sea Wave Energy Converter system (ISWEC), developed by the DIMEAS Department at Politecnico di Torino (G.Bracco, E.Giorcelli, G.Mattiazzo), that using the gyroscopic effect is able to drive a Power Take Off system (PTO) converting mechanical power into electrical power. This new project allows to avoid the corrosion by the sea of the system components, using a monolithic float that contains inside it the gyroscopic system and all the important parts ([3]). In order to produce power, a reaction force to damp the PTO motion, and a respective control strategy are needed. Different control strategies are considered to aim that problem, as PD ([5]) and MPC ([6]). The new scope of finding solution through Robust Control approach is my interested object, in order to reach a new solution that can provide a useful instrument in the ISWEC system, and thinking big, to the RES engineering studies.

## Thesis organization

The main software used in thesis work is Matlab/Simulink. The tools used for the Set Membership Identification are SparsePOP and SeDuMi, while the research of the controller is done with lmi optimization package.

The thesis is organized in 5 chapters: the first chapter analyze in detail the main ISWEC system concepts, the second and the third chapters show the Set Membership and the  $H_\infty$  controller theory and simulations, the fourth analyzes the non linear validation developed and the new better results, finally the chapter 5 with the conclusion of the entire work.



# Chapter 1

## Iswec system

### Introduction

The ISWEC system (Inertial Sea Wave Energy Converter) is born in the DIMEAS Department at Politecnico di Torino to produce electrical power through the gyroscopic effect of a flywheel, as can be seen in more accurate way in the article [3]. The project is studied for Mediterranean environment, that with respect to oceans, is characterized by lower average wave power and higher frequency. The layout (1.1) is composed by a monolithic floating hull, with an inner room sealed from the outer environment.

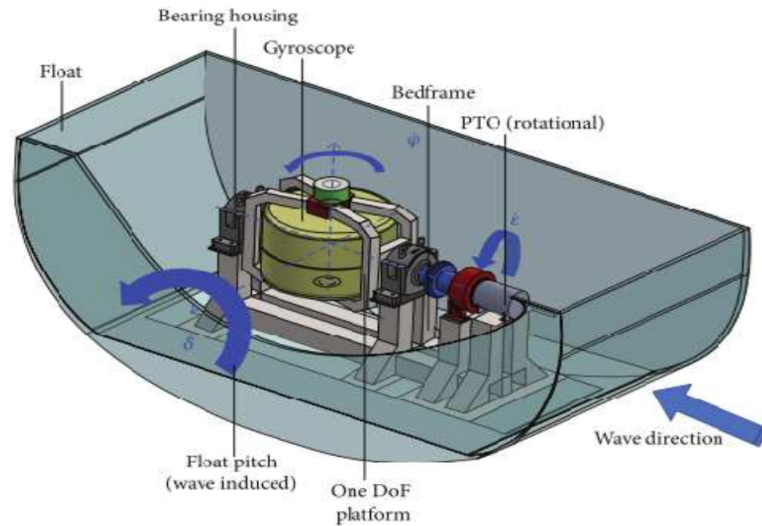


Figure 1.1: *ISWEC layout*.

In the internal room are present the two gyroscopes, the PTO unit (Power Take Off) and the power conditioning system. Thanks to the slack mooring configuration of the floater mooring system, the hull is self aligning with respect to the incoming wave, such that the wave contribution can be induced on the float pitch angle, as shown in figure 1.1.

In order to produce energy, the gyroscopic effect and the precession motion concepts are used. The gyroscopic system includes a flywheel connected to the shaft. Considering the axis configuration shown in figure 1.1, a motor takes in rotation the flywheel around Z-axis (with an angular velocity of  $\dot{\varphi}$ ) that combined with the wave induced pitch velocity  $\dot{\delta}$ , allows the flywheel to rotate around X-axis through the gyroscopic effect, generating a torque along  $\varepsilon$ . Damping the precession motion with a torque  $T_\varepsilon$  around coordinate  $\varepsilon$ , the energy is produced. The dynamical equations are the following:

1.

$$T_\varepsilon(t) = I_g \ddot{\varepsilon}(t) - (J - I_g) \dot{\delta}^2(t) \sin(\varepsilon(t)) \cos(\varepsilon(t)) + J \dot{\varphi}(t) \dot{\delta}(t) \cos(\varepsilon(t)) \quad (1.1)$$

$\downarrow$

$$T_\varepsilon(t) \approx I_g \ddot{\varepsilon}(t) + J \dot{\varphi}(t) \dot{\delta}(t) \cos(\varepsilon(t)) \quad (1.2)$$

Dynamic behavior on axis  $\varepsilon$ :

- $T_\varepsilon$ : PTO torque;
- $I_g$ : total moment of inertia with respect to PTO  $\varepsilon$ -axis;
- $J$ : gyroscope axis-symmetric moment of inertia;
- $\dot{\varphi}$ : flywheel angular speed.

2.

$$T_\delta(t) = (I_g \cos^2(\varepsilon(t)) + J \sin^2(\varepsilon(t))) \ddot{\delta}(t) + 2(J - I_g) \dot{\delta}(t) \dot{\varepsilon}(t) \sin(\varepsilon(t)) \cos(\varepsilon(t)) + J \dot{\varphi}(t) \dot{\varepsilon}(t) \cos(\varepsilon(t)) - J \ddot{\varphi}(t) \sin(\varepsilon(t)) \quad (1.3)$$

$\downarrow$

$$T_\delta(t) \approx -J \dot{\varphi}(t) \dot{\varepsilon}(t) \cos(\varepsilon(t)) \quad (1.4)$$

- $T_\delta$ : applied torque to the gyroscopic system

The equations 1.1 and 1.3 represents the extended version of dynamical behavior, while the equations 1.2 and 1.4 represent the approximated relations considering the working conditions of ISWEC system in Mediterranean Sea. Furthermore, considering the self orientating property of the system described before, the floater dynamical equation can be described by the Cummins' equation:

$$\tau_w(t) = (I_{eq} + \mu_\infty) \ddot{\delta}(t) + \beta |\dot{\delta}(t)| \dot{\delta}(t) + K_w \delta(t) + T_\delta(t) + \int_0^t \dot{\delta}(\tau) h(t - \tau) d\tau \quad (1.5)$$

- $\tau_w$ : wave induced torque on the floater;
- $I_{eq}$ : system moment of inertia around  $\delta$ ;
- $\mu_\infty$ : instantaneous added mass;

- $K_w$ : linear hydrostatic stiffness;
- $\beta$ : Morison viscous quadratic coefficient.

The hydrodynamics radiation force memory effects are described by the following convolution integral:

$$\mu(t) = \int_0^t \dot{\delta}(\tau)h(t-\tau)d\tau \quad (1.6)$$

## Linear model

In order to take the necessary dataset for Set-Membership Identification, the MPC control model is considered, so are shown the linearized equations necessary for the MPC design.

The first consideration is to assume the flywheel speed set to a constant value, so  $\varepsilon = \delta = 0$  and the eq.1.2 can be schematized as follow:

$$T_\varepsilon(t) = I_g \ddot{\varepsilon}(t) + J\bar{\varphi}\dot{\delta}(t) \quad (1.7)$$

Introducing the radiation force dynamical state as:

$$\rho_{rv}(t) = [\rho_{rv,1}(t) \quad \dots \quad \rho_{rv,v}(t)]^\top \in \mathbb{R}^\nu \quad (1.8)$$

and the matrices  $A_\rho$ ,  $B_\rho$  and  $C_\rho$  as:

$$A_\rho = \begin{bmatrix} a_1 & a_2 & \dots & a_v \\ 1 & 0 & \dots & 0 \\ \vdots & \ddots & 0 & 0 \\ 0 & 0 & 1 & 0 \end{bmatrix} \quad (1.9)$$

$$B_\rho = \begin{bmatrix} 1 \\ 0 \\ \vdots \\ 0 \end{bmatrix} \quad (1.10)$$

$$C_\rho = [c_1 \quad c_2 \quad \dots \quad c_v] \quad (1.11)$$

the convolution integral defined before in 1.6 can be defined as follows:

$$\mu(t) = \int_0^t \dot{\delta}(\tau)h(t-\tau)d\tau \approx \begin{cases} \dot{\rho}_{rv}(t) = A_\rho \rho_{rv}(t) + B_\rho \dot{\delta}(t) \\ \mu(t) = C_\rho \rho_{rv}(t) \end{cases} \quad (1.12)$$

The Cummins' equation 1.5 becomes:

$$\tau_w(t) = (I_{eq} + \mu_\infty) \ddot{\delta}(t) + K_w \delta(t) - J\bar{\varphi} \dot{\varepsilon}(t) + C_\rho \rho_{rv}(t) \quad (1.13)$$

Considering the state variable

$$x(t) = \begin{bmatrix} \dot{\varepsilon}(t) & \varepsilon(t) & \dot{\delta}(t) & \delta(t) & \rho_{rv,1}(t) & \dots & \rho_{rv,\nu}(t) \end{bmatrix}^\top \in \mathbb{R}^{4+\nu} \quad (1.14)$$

the total linearized model of the ISWEC system can be described by the state equation 1.15:

$$\dot{x}(t) = Ax(t) + BT_\varepsilon(t) + B^\tau \tau_w(t) \quad (1.15)$$

The matrix  $A$ ,  $B$  and  $B^\tau$  are:

$$A = \begin{bmatrix} 0 & 0 & \frac{-J\bar{\varphi}}{I_g} & 0 & 0 & 0 & \dots & 0 \\ 1 & 0 & 0 & 0 & 0 & 0 & \dots & 0 \\ \frac{J\bar{\varphi}}{I_{eq}^*} & 0 & 0 & \frac{-K_w}{I_{eq}^*} & \frac{-c_1}{I_{eq}^*} & \frac{-c_2}{I_{eq}^*} & \dots & \frac{-c_v}{I_{eq}^*} \\ 0 & 0 & 1 & 0 & 0 & 0 & \dots & 0 \\ 1 & 0 & 0 & 0 & a_1 & a_2 & \dots & a_v \\ 0 & 0 & 0 & 0 & 1 & 0 & \dots & 0 \\ \vdots & \vdots & \vdots & \vdots & \vdots & \ddots & 0 & 0 \\ 0 & 0 & 0 & 0 & 0 & 0 & 1 & 0 \end{bmatrix} \quad (1.16)$$

$$B = \left[ \frac{1}{I_g} \quad 0 \quad 0 \quad 0 \quad 0 \quad 0 \quad \dots \quad 0 \right]' \quad (1.17)$$

$$B^\tau = \left[ 0 \quad 0 \quad \frac{1}{I_{eq}^*} \quad 0 \quad 0 \quad 0 \quad \dots \quad 0 \right]' \quad (1.18)$$

with  $I_{eq}^* = I_{eq} + \mu_\infty$ .

The power extracted by the system is:

$$P_{PTO}(t) = \dot{\varepsilon}(t) \cdot T_\varepsilon(t)$$

The convention used considers as released power a positive quantity, so the power absorbed is  $-P_{PTO}$ .

## Chapter 2

# Set membership identification

In this chapter a brief review of main fundamental results on Set-membership identification theory is reported for self-consistency. The interested reader can find details in the following papers [7], [8] and [9].

### 2.1 Basic notions

The identification object is to evaluate a model through a set of given information. The identified system can be:

- *static*: output at time  $t_0$  depends only on input at time  $t_0$
- *dynamic*: output at time  $t_0$  depends on input at time  $t_0$  and by past input values

Using the regression form, the obtained model is the following:

$$w(t) = f(w(t-1), w(t-2), \dots, w(t-n), u(t), u(t-1), \dots, u(t-n))$$

where  $w(t)$  is the output at time  $t$  and  $u(t)$  is the input at time  $t$ .

The model can be classified in:

- *parametric*: defined by a finite number of parameters
- *non parametric*: defined by an infinite number of parameters

The objective is to find a *linear* system, in order to obtain an output as linear combination of the other variables:

$$w(t) = \alpha_1 w(t-1) + \dots + \alpha_n w(t-n) + \beta_0 u(t) + \dots + \beta_m u(t-m)$$

The goal followed in the thesis work is to find a discrete, parametric, linear time-invariant model (LTI).

#### 2.1.1 Error representation

There are different ways in order to take into account the noise affecting the system.

The main topologies are:

1. *Equation error*: the noise effect is taken into account by means of an eq.error

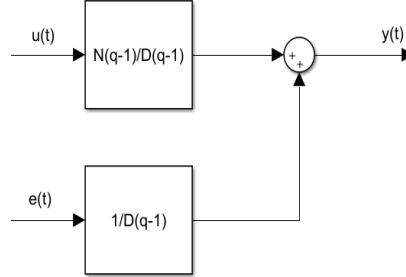


Figure 2.1: *Eq.error structure.*

2. *Error-in-variable*: the error noise affects both input and output(  $u(t)$  and  $w(t)$  are real input and output,  $\eta(t)$  and  $\epsilon(t)$  are the noise contribution,  $\tilde{u}(t)$  and  $y(t)$  the collected data)

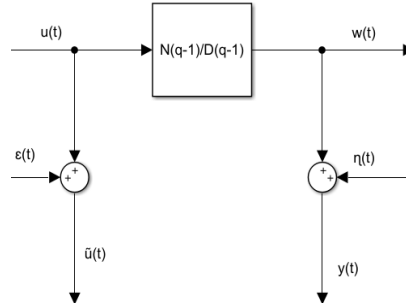


Figure 2.2: *Errors in variables structure.*

3. *Output error*: the input signal is assumed to be known, while the output sequence is corrupted by error  $\eta(t)$

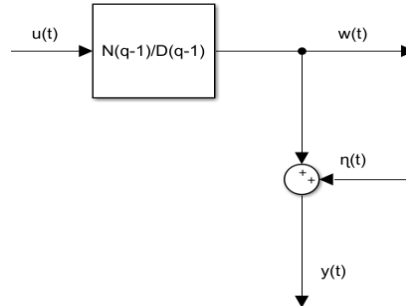


Figure 2.3: *Output error structure.*

Concerning the errors  $\varepsilon(t)$  and  $\eta(t)$ , the two methodologies to be considered are:

- *Statistical*:  $\varepsilon(t)$  and  $\eta(t)$  are random variable statistically distributed with a probability density function totally or partially known;
- *Set-membership bounded error*:  $\varepsilon(t)$  and  $\eta(t)$  have unknown behaviour but are limited and belong to a given bounded set.

$$|\eta(t)| \leq \Delta\eta, \forall t = 1, \dots, N$$

$$|\varepsilon(t)| \leq \Delta\varepsilon, \forall t = 1, \dots, N$$

$$\Delta\eta, \Delta\varepsilon \text{ are known}$$

### 2.1.2 Feasible Parameter Set and Polynomial optimization problem

In the set-membership identification, the *feasible solution set* (FSS) is the set of all the models which are feasible solutions of the estimated problem. If the class of system  $F$  is parametrized by a parameter vector  $\Theta$ , the FSS can be replaced by the feasible parameter set.

The *feasible parameter set*  $D_\theta$  (FPS) is the set of all the parameter values that satisfies the model equations, given for all the collected input/output data and corrupted by bounded noise.

Considering as error structure the output error representation, the FPS describing the model is:

$$D_\theta = \{\theta = [\alpha_1, \dots, \alpha_n, \beta_0, \dots, \beta_n] \in \mathbb{R}^{2n+1} : \quad (2.1)$$

$$w(t) = -\alpha_1 w(t-1) - \dots - \alpha_n w(t-n) + \beta_0 u(t) + \dots + \beta_n u(t-n) \quad (2.2)$$

$$y(t) = w(t) + \eta(t) \quad (2.2)$$

$$|\eta(t)| \leq \Delta\eta, \quad \forall t = 1, \dots, N\}$$

Substituting the 2.2 in 2.1, it is possible to obtain the *extended feasible parameter set* (EFPS), defined by a set of bilinear equality constraints and by a set of linear inequality constraint:

$$D_{\theta, \eta} = \{\theta = [\alpha_1, \dots, \alpha_n, \beta_0, \dots, \beta_n] \in \mathbb{R}^{2n+1}, \eta \in \mathbb{R}^N : \quad (2.3)$$

$$y(t) - \eta(t) = -\alpha_1 (y(t-1) - \eta(t-1)) - \dots - \alpha_n (y(t-n) - \eta(t-n)) + \beta_0 u(t) + \dots + \beta_n u(t-n) \quad (2.4)$$

$$|\eta(t)| \leq \Delta\eta, \quad \forall t = 1, \dots, N\}$$

The previous equations allow to find the interval of each parameter value, determining the *parameter uncertainty interval* (PUI).

The PUI of a parameter value is the interval of its values, limited by minimum and maximum.

$$PUI_{\theta_i} = [\underline{\theta}_i, \bar{\theta}_i]$$

$$\underline{\theta}_i = \min \theta_i$$

subject to

$$y(t) - \eta(t) = -\alpha_1 y(t-1) + \alpha_1 \eta(t-1) + \dots + \beta_0 u(t) + \dots + \beta_n u(t-n) \quad \forall t = n+1, \dots, N \quad (2.5)$$

$$-\Delta\eta \leq \eta(t) \leq \Delta\eta \quad \forall t = 1, \dots, N \quad (2.6)$$

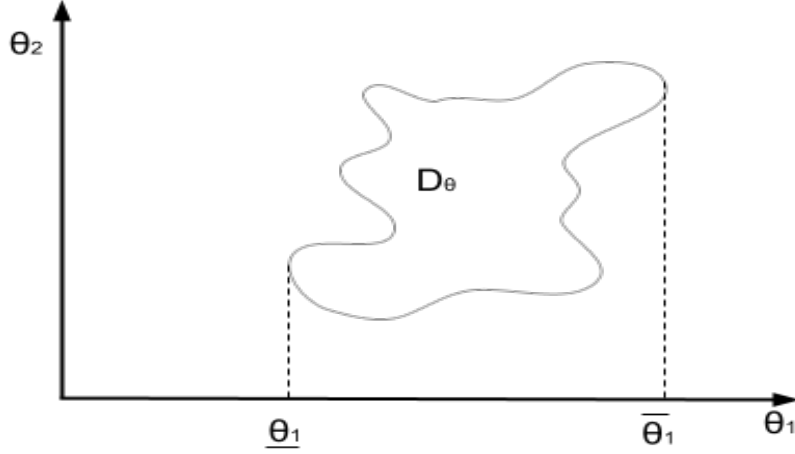


Figure 2.4: *Parameter uncertainty interval.*

Due to the presence of bilinear equality constraints in the equation 2.5, it is possible to define the problem as "bilinear optimization problem", a subclass of *polynomial optimization problem*.

A *polynomial optimization problem*(POP) is an optimization problem in the following general form:

$$\min f(x)$$

subject to

$$y_i(x) \geq 0 \quad \forall i = 1, \dots, \Gamma$$

where  $x$ =decision/optimization variables of the problem,  $f(x)$  is a multivariate polynomial function of the decision variable  $x$ .

The main features of POPs are the following:

- Non linear optimization problems
- Non convex optimization problems

Due to the non-convexity, the problem could have more local minimum solutions, so in order to care of these constraints, a good method is to compute an "outer approximation" of the PUI. In this way, the computed PUI is not numerically exact, due to the added conservativeness, but it is possible to guarantee that the true plant



is inside the considered set.

The POP problem can be rewritten as follows:

$$\min \gamma$$

subject to

$$\begin{aligned} f(x) &\leq \gamma \quad \rightarrow \quad \gamma - f(x) \geq 0 \\ g_i(x) &\geq 0 \quad \forall i = 1, \dots, \Gamma \\ g_j(x) &\geq 0 \quad \forall j = 1, \dots, M \end{aligned} \tag{2.7}$$

The problem 2.7 can be seen as the minimization of a linear function of the optimization variable, subject to a set of polynomial constraints. In order to solve this problem, the idea is to use convex relaxation methods.

The *convex relaxation methods* are based on the idea of approximating the non-convex set, described by the polynomial constraints in 2.7, with a convex set which includes the non convex original one.

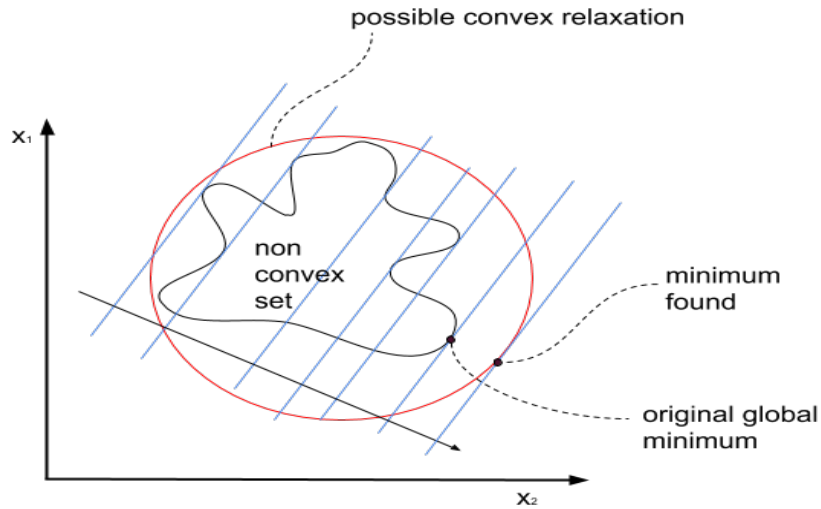


Figure 2.5: *Convex relaxation scheme.*

The approach is to consider the non-convex set depending on a parameter called *order of relaxation*  $\delta$ :

1. As  $\delta \rightarrow \infty$  the convex approximation tends to the *convex hull* of the original non convex set
2. As  $\delta$  increases, the computational cost grows exponentially

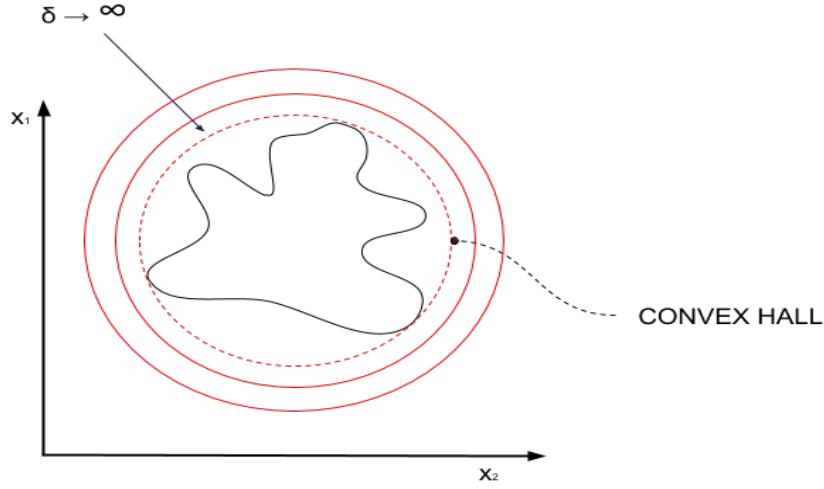


Figure 2.6: *Convex hall*.

The *convex hall* of a set  $S$  is the smallest outer approximation of the original set  $S$ . The minimum possible value of  $\delta$  ( $\delta_{min}$ ), is given by:

$$\delta_{min} = \lceil \frac{\max \text{ degree}}{2} \rceil$$

where max degree is the maximum degree of the polynomial describing the objective function and the constraints.

### 2.1.3 SparsePOP tool

The instrument used to solve POPs is *SparsePOP*, exploited in this article [10]. *SparsePOP* is a Matlab package, used in order to find global optimal solutions of POPs. The POP is written in the following form:

$$\begin{aligned} & \text{minimize } f_0(x) \\ & \text{subject to} \\ & f_k(x) \geq 0 \quad (k = 1, 2, \dots, l), \\ & f_k(x) = 0 \quad (k = l + 1, \dots, m), \\ & lbd_i \leq x_i \leq ubd_i \quad (i = 1, 2, \dots, n) \end{aligned}$$

where  $-\infty \leq lbd_i < \infty$  and  $-\infty < ubd_i \leq \infty$  ( $i=1,2,\dots,n$ ). The package input is a polynomial optimization problem, so constructing a sparse semidefinite programming (SDP) relaxation of the POP, gives as output solution information and statistics. The solver used by Matlab to solve the SDP can be SDPA or SeDuMi, providing an approximate global optimal solution.

In SparsePOP, a polynomial class is defined as follows:

**poly.typeCone** = 1 if  $f(x) \in \mathbb{R}[x]$  is used as an objective function  
 = 1 if  $f(x) \in \mathbb{R}[x]$  is used as  $f(x) \geq 0$   
 = -1 if  $f(x) \in \mathbb{R}[x]$  is used as  $f(x) = 0$   
**poly.degree** = the degree of  $f(x)$   
**poly.dimVar** = the dimension of variable vector  $x$   
**poly.noTerms** = the number of terms of  $f(x)$   
**poly.supports** = support set of  $f(x)$ , a  $\text{poly.noTerms} \cdot \text{poly.dimVar}$  matrix  
**poly.coef** = coefficients, a column vector of  $\text{poly.noTerms}$  dimension

The name *objPoly* is for the objective polynomial function  $f_0(x)$  and *ineqPolySysj* ( $j=1,2,\dots,m$ ) for the polynomials  $f_1(x)$  ( $j=1,2,\dots,m$ ) of the constraints.

The package allows also to find an approximation to an optimal solution, setting the *param.POPsolver* to "active-set" (this function is possible only if an Optimization Toolbox is available in Matlab).

## 2.2 Set-membership in ISWEC model

### 2.2.1 Model requirements

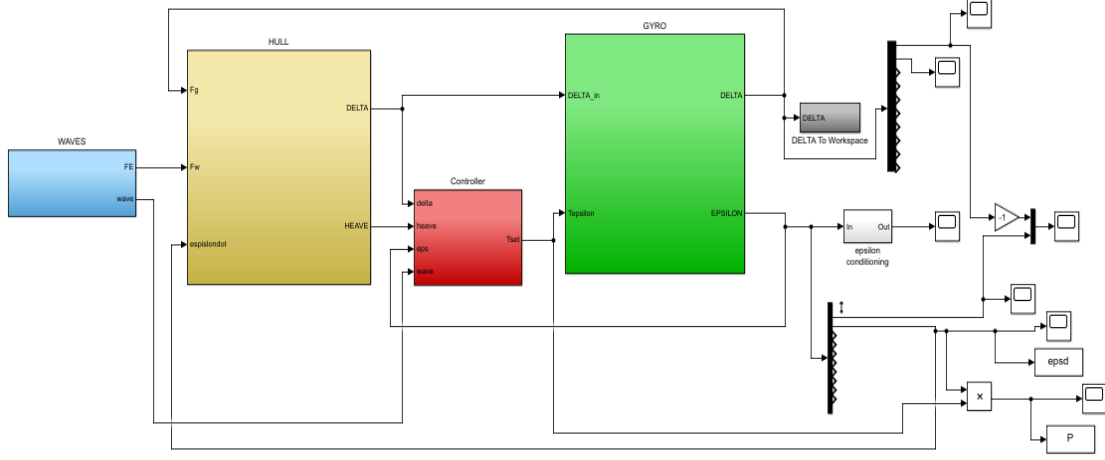
The main goal is to identify a good model that can represent the ISWEC plant. As described in previous section, the necessary information in order to apply the set-membership identification, are:

- a set of a-priori information of the system
- a set of input-output data of the plant
- the noise structure

In the thesis work, the system to be identified is assumed to be a linear time-invariant system.

The idea is to identify a model that takes care of both the internal dynamic contribution and the external contribution given by the incoming wave. In order to satisfy these requirements, the first input is the torque delivered by the PTO unit  $T_\varepsilon$ , while the second input is the incoming wave force contribution to the rotation on pitch axis *Fry*. The chosen output is the angular speed of the PTO shaft  $\dot{\varepsilon}$ .

In order to collect the set of input-output data, an old project with MPC controller is considered.


 Figure 2.7: *Iswec MPC*.

As can be seen in the figure 2.7, the torque  $T_\epsilon$  is the output of controller block, the angular speed  $\dot{\epsilon}$  is the output of gyroscope block, while the wave force contribution is taken from the waves block. The data are taken considering 4 different wave profiles, which give a linear profile of  $\dot{\epsilon}$  as output in the MPC model. The MPC system is constructed considering the 8 states (1.14).

Concerning the number of states in the two transfer functions, it must be considered that higher is the number of states and better should be the represented system behaviour, but the problem complexity increases exponentially.

In the thesis work are shown two different approaches, the first considering a transfer function with nine states, while the second considering the transfer function of second degree.

The error structure considered is the output error, in order to consider the error between the real and simulated output.

Knowing the previous information, the model structure is the following:

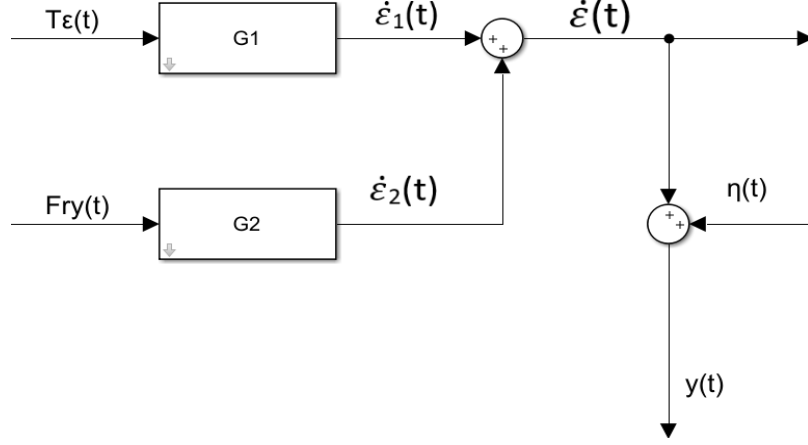


Figure 2.8: *Model structure.*

The plant model is:

$$G_1(q^{-1}) = \frac{\dot{\varepsilon}_1(z)}{T_\varepsilon} = \frac{\beta_{10} + \dots + \beta_{1n}q^{-n}}{1 + \alpha_{11}q^{-1} + \dots + \alpha_{1n}q^{-n}} \quad (2.8)$$

The disturbance model, that takes into account the wave contribution, is:

$$G_2(q^{-1}) = \frac{\dot{\varepsilon}_2(z)}{F_{ry}} = \frac{\beta_{20} + \dots + \beta_{2n}q^{-n}}{1 + \alpha_{21}q^{-1} + \dots + \alpha_{2n}q^{-n}} \quad (2.9)$$

Considering the model structure shown in figure 2.8, it is possible to see that the angular speed of PTO shaft is given by the contribution of the two transfer functions:

$$\dot{\varepsilon}(t) = \dot{\varepsilon}_1(t) + \dot{\varepsilon}_2(t) \quad (2.10)$$

The output  $y(t)$  is simulated output, given from the sum of real output  $\dot{\varepsilon}$  and of error  $\eta(t)$ .

$$y(t) = \dot{\varepsilon}(t) + \eta(t) \quad \rightarrow \quad y(t) = \dot{\varepsilon}_1(t) + \dot{\varepsilon}_2(t) + \eta(t) \quad (2.11)$$

where  $\eta(t)$  is bounded

$$|\eta(t)| \leq \Delta\eta \quad (2.12)$$

From the previous equations, it is possible to proceed to the SparsePOP problem. Due to the final goal of the work, the SparsePOP minimization will be done in order to minimize the error  $\eta(t)$ , so the parameters will be referred to the minimum calculated error.

In the next sections will be shown a second degree and a nine degree system identification, which have very similar results in SM identification, but very different in H-inf approach.

## 2.2.2 Low order model identification

### 2.2.2.1 Identification

Considering two states, the plant transfer function and the disturbance transfer function are :

$$G_1(q^{-1}) = \frac{\dot{\varepsilon}_1(t)}{T_\varepsilon(t)} = \frac{\beta_{10} + \beta_{11}q^{-1} + \beta_{12}q^{-2}}{1 + \alpha_{11}q^{-1} + \alpha_{12}q^{-2}} \quad (2.13)$$

$$G_2(q^{-1}) = \frac{\dot{\varepsilon}_2(t)}{F_{ry}(t)} = \frac{\beta_{20} + \beta_{21}q^{-1} + \beta_{22}q^{-2}}{1 + \alpha_{21}q^{-1} + \alpha_{22}q^{-2}} \quad (2.14)$$

From the 2.13 and 2.14 it is possible to define the equality constraints of the problem:

$$\begin{aligned} \dot{\varepsilon}_1(t)(1 + \alpha_{11}q^{-1} + \alpha_{12}q^{-2}) &= T_\varepsilon(t)(\beta_{10} + \beta_{11}q^{-1} + \beta_{12}q^{-2}) \\ \dot{\varepsilon}_1(t) + \alpha_{11}\dot{\varepsilon}_1(t-1) + \alpha_{12}\dot{\varepsilon}_1(t-2) &= \beta_{10}T_\varepsilon(t) + \beta_{11}T_\varepsilon(t-1) + \beta_{12}T_\varepsilon(t-2) \\ \dot{\varepsilon}_1(t) + \alpha_{11}\dot{\varepsilon}_1(t-1) + \alpha_{12}\dot{\varepsilon}_1(t-2) - \beta_{10}T_\varepsilon(t) - \beta_{11}T_\varepsilon(t-1) - \beta_{12}T_\varepsilon(t-2) &= 0 \end{aligned} \quad (2.15)$$

The equation 2.15 is the first system equation.

Following the same procedure for the disturbance transfer function, the result is:

$$\begin{aligned} \dot{\varepsilon}_2(t)(1 + \alpha_{21}q^{-1} + \alpha_{22}q^{-2}) &= F_{ry}(t)(\beta_{20} + \beta_{21}q^{-1} + \beta_{22}q^{-2}) \\ \dot{\varepsilon}_2(t) + \alpha_{21}\dot{\varepsilon}_2(t-1) + \alpha_{22}\dot{\varepsilon}_2(t-2) &= \beta_{20}F_{ry}(t) + \beta_{21}F_{ry}(t-1) + \beta_{22}F_{ry}(t-2) \\ \dot{\varepsilon}_2(t) + \alpha_{21}\dot{\varepsilon}_2(t-1) + \alpha_{22}\dot{\varepsilon}_2(t-2) - \beta_{20}F_{ry}(t) - \beta_{21}F_{ry}(t-1) - \beta_{22}F_{ry}(t-2) &= 0 \end{aligned} \quad (2.16)$$

The equation 2.16 is the second system equation.

The relation that links 2.15 and 2.16 to the real output(angular speed) is the following:

$$\dot{\varepsilon}(t) = \dot{\varepsilon}_1(t) + \dot{\varepsilon}_2(t) \quad (2.17)$$

The parameters  $\dot{\varepsilon}_1(t)$  and  $\dot{\varepsilon}_2(t)$  are the partial outputs of the two transfer functions, unknown, from which the sum gives the real output(PTO shaft angular speed). Considering the equations 2.15, 2.16, 2.17 and 2.12, it is possible to proceed to the *extended feasible parameter set(EFPS)*:

$$D_{\theta, \dot{\varepsilon}_1, \dot{\varepsilon}_2, \Delta\eta} = \{\theta = [\alpha_{11}, \alpha_{12}, \alpha_{21}, \alpha_{22}, \beta_{10}, \beta_{11}, \beta_{12}, \beta_{20}, \beta_{21}, \beta_{22}] \in \mathbb{R}^{10},$$

$$\dot{\varepsilon}_1 \in \mathbb{R}^N, \dot{\varepsilon}_2 \in \mathbb{R}^N, \Delta\eta \in \mathbb{R}^1 :$$

$$\begin{aligned} \dot{\varepsilon}_1(t) + \alpha_{11}\dot{\varepsilon}_1(t-1) + \alpha_{12}\dot{\varepsilon}_1(t-2) - \beta_{10}T_\varepsilon(t) - \beta_{11}T_\varepsilon(t-1) - \beta_{12}T_\varepsilon(t-2) &= 0 \\ \dot{\varepsilon}_2(t) + \alpha_{21}\dot{\varepsilon}_2(t-1) + \alpha_{22}\dot{\varepsilon}_2(t-2) - \beta_{20}F_{ry}(t) - \beta_{21}F_{ry}(t-1) - \beta_{22}F_{ry}(t-2) &= 0 \\ y(t) = \dot{\varepsilon}_1(t) + \dot{\varepsilon}_2(t) + \eta(t) &\rightarrow \eta(t) = y(t) - \dot{\varepsilon}_1(t) - \dot{\varepsilon}_2(t) \end{aligned} \quad (2.18)$$

$$|\eta(t)| \leq \Delta\eta \quad (2.19)$$

Substituting the equation 2.18 into equation 2.19 and evolving the inequality, it is possible to obtain:

$$D_{\theta, \varepsilon_1, \varepsilon_2, \Delta\eta} = \{\theta = [\alpha_{11}, \alpha_{12}, \alpha_{21}, \alpha_{22}, \beta_{10}, \beta_{11}, \beta_{12}, \beta_{20}, \beta_{21}, \beta_{22}] \in \mathbb{R}^{10},$$

$$\dot{\varepsilon}_1 \in \mathbb{R}^N, \dot{\varepsilon}_2 \in \mathbb{R}^N, \Delta\eta \in \mathbb{R}^1 :$$

$$\dot{\varepsilon}_1(t) + \alpha_{11}\dot{\varepsilon}_1(t-1) + \alpha_{12}\dot{\varepsilon}_1(t-2) - \beta_{10}T_\varepsilon(t) - \beta_{11}T_\varepsilon(t-1) - \beta_{12}T_\varepsilon(t-2) = 0 \quad (2.20)$$

$$\dot{\varepsilon}_2(t) + \alpha_{21}\dot{\varepsilon}_2(t-1) + \alpha_{22}\dot{\varepsilon}_2(t-2) - \beta_{20}F_{ry}(t) - \beta_{21}F_{ry}(t-1) - \beta_{22}F_{ry}(t-2) = 0 \quad (2.21)$$

$$y(t) - \dot{\varepsilon}_1(t) - \dot{\varepsilon}_2(t) \leq \Delta\eta \quad \rightarrow \quad \Delta\eta - y(t) + \dot{\varepsilon}_1(t) + \dot{\varepsilon}_2(t) \geq 0, \quad \forall t = 1, \dots, N \quad (2.22)$$

$$-y(t) + \dot{\varepsilon}_1(t) + \dot{\varepsilon}_2(t) \leq \Delta\eta \quad \rightarrow \quad \Delta\eta + y(t) - \dot{\varepsilon}_1(t) - \dot{\varepsilon}_2(t) \geq 0, \quad \forall t = 1, \dots, N \quad (2.23)$$

The previous table shows the two equality constraints (2.20, 2.21) and the two inequality constraints 2.22, 2.23, so it is possible now to proceed to the the SparsePOP execution in order to solve the problem.

The objective function, in that case, is to minimize the error  $\Delta\eta$  and to find the respective parameter values.

The first step is to define the **objPoly**:

```

objPoly.typeCone = 1, because it is an objective function
objPoly.degree = 1, degree of  $\Delta\eta$ 
objPoly.dimVar = 11+2N, 10 variables +  $\Delta\eta$  + N variables  $\dot{\varepsilon}_1$  + N
variables  $\dot{\varepsilon}_2$ 
objPoly.noTerms = 1, the objective function is formed by only one
term
objPoly.supports = zeros(1,11+2N)
objPoly.supports(1,11) = 1
objPoly.coef = 1, the objective is to find only the minimum error pa-
rameter
    
```

The highest equation degree is 2, so the parameter *tmin* is 3. The number of samples considered in the final simulation is 100, upon the total 3001 samples of each data. The first equality constraint is analyzed as follow:

$$\dot{\varepsilon}_1(t) + \alpha_{11}\dot{\varepsilon}_1(t-1) + \alpha_{12}\dot{\varepsilon}_1(t-2) - \beta_{10}T_\varepsilon(t) - \beta_{11}T_\varepsilon(t-1) - \beta_{12}T_\varepsilon(t-2) = 0$$

```

ineqPolySys{t-tmin+1}.typeCone = -1;
ineqPolySys{t-tmin+1}.degree = 2;
ineqPolySys{t-tmin+1}.dimVar = 11+2N;
ineqPolySys{t-tmin+1}.noTerms = 6;
ineqPolySys{t-tmin+1}.supports = A;
A = zeros(6, 11+2N); A(1,11+t) = 1; A(2,1) = 1; A(2,11+t-1) = 1; A(3,2) = 1;
A(3,11+t-2) = 1; A(4,3) = 1; A(5,4) = 1; A(6,5) = 1;
ineqPolySys{t-tmin+1}.coef = [ones(1,3) - T(t) - T(t-1) - T(t-2)]';
    
```

The second equality constraint is analyzed as follows:

$$\dot{\varepsilon}_2(t) + \alpha_{21}\dot{\varepsilon}_2(t-1) + \alpha_{22}\dot{\varepsilon}_2(t-2) - \beta_{20}F_{ry}(t) - \beta_{21}F_{ry}(t-1) - \beta_{22}F_{ry}(t-2) = 0$$

```

ineqPolySys{t-2*tmin+N+2}.typeCone=-1;
ineqPolySys{t-2*tmin+N+2}.degree= 2;
ineqPolySys{t-2*tmin+N+2}.dimVar=11+2N;
ineqPolySys{t-2*tmin+N+2}.noTerms=6;
ineqPolySys{t-2*tmin+N+2}.supports=B;
B=zeros(6, 11+2N); B(1,11+N+t)=1; B(2,6)=1; B(2,11+N+t-1)=1; B(3,7)=1;
  B(3,11+N+t-2)=1; B(4,8)=1; B(5,9)=1; B(6,10)=1;
ineqPolySys{t-tmin+1}.coef=[ones(1,3) - F(t) - F(t-1) - F(t-2)]';

```

The first inequality constraint is analyzed as follows:

$$\Delta\eta - y(t) + \dot{\varepsilon}_1(t) + \dot{\varepsilon}_2(t) \geq 0$$

```

ineqPolySys{t-3*tmin+2*N+3}.typeCone=1;
ineqPolySys{t-3*tmin+2*N+3}.degree= 1;
ineqPolySys{t-3*tmin+2*N+3}.dimVar=11+2N;
ineqPolySys{t-3*tmin+2*N+3}.noTerms=4;
ineqPolySys{t-3*tmin+2*N+3}.supports=C;
C=zeros(4, 11+2N); C(1,11+t)=1; C(2,11+N+t)=1; C(4,11)=1;
ineqPolySys{t-3*tmin+2*N+3}.coef=[11 - y(t)1]';

```

The second inequality constraint is analyzed as follows:

$$\Delta\eta + y(t) - \dot{\varepsilon}_1(t) - \dot{\varepsilon}_2(t) \geq 0$$

```

ineqPolySys{t-4*tmin+3*N+4}.typeCone=1;
ineqPolySys{t-4*tmin+3*N+4}.degree= 1;
ineqPolySys{t-4*tmin+3*N+4}.dimVar=11+2N;
ineqPolySys{t-4*tmin+3*N+4}.noTerms=4;
ineqPolySys{t-4*tmin+3*N+4}.supports=D;
D=zeros(4, 11+2N); D(1,11+t)=1; D(2,11+N+t)=1; D(4,11)=1;
ineqPolySys{t-4*tmin+3*N+4}.coef=[-1 - 1y(t)1]';

```

The support matrix is the same of first inequality constraint.

The lower bound and upper bound are considered as following:

$$lbd = [-1e10ones(1,11+2N)];$$

$$ubd = [1e10ones(1,11+2N)];$$

Considering the highest degree as 2, the param.relaxOrder is 1. In order to find the optimal solution, the param.POPsolver is set to "active-set".



In order to find the minimum error  $\Delta\eta$ (objective function) and the associated parameter values, the following code is used:

```
[~,~,POP]=sparsePOP(objPoly,ineqPolySys,lbd,ubd,param);
delta_eta = POP.xVect(11);
for j=1:10
    th(j)=POP.xVect(j);
end
delta_etaL = POP.xVectL(11);
for j=1:10
    thL(j)=POP.xVectL(j);
end
```

where "L" indicates the parameters found as optimal solution.

The plant and disturbance transfer functions, corresponding to the non-optimal solution and optimal solution, are found considering the Z-domain transfer functions:

$$\begin{aligned}
 Gp_z &= \frac{th(3)z^2 + th(4)z + th(5)}{z^2 + th(1)z + th(2)} \\
 Gd_z &= \frac{th(8)z^2 + th(9)z + th(10)}{z^2 + th(6)z + th(7)} \\
 Gp_z_L &= \frac{thL(3)z^2 + thL(4)z + thL(5)}{z^2 + thL(1)z + thL(2)} \\
 Gd_z_L &= \frac{thL(8)z^2 + thL(9)z + thL(10)}{z^2 + thL(6)z + thL(7)}
 \end{aligned} \tag{2.24}$$

In order to work with the two transfer functions in the the next chapter, a continuous transfer function has to be found. The Matlab command *d2c* is used to obtain the corresponding transfer functions in the Laplace domain.

The SparsePOP solution is found for each wave dataset, obtaining four couple of transfer functions.

### 2.2.2.2 Identification results

In this part are shown the better solutions of the SparsePOP identification. The first identified transfer functions are corresponding to the wave profile 3. It is possible to compare the different outputs obtained, with respect to the real output obtained by the MPC model.

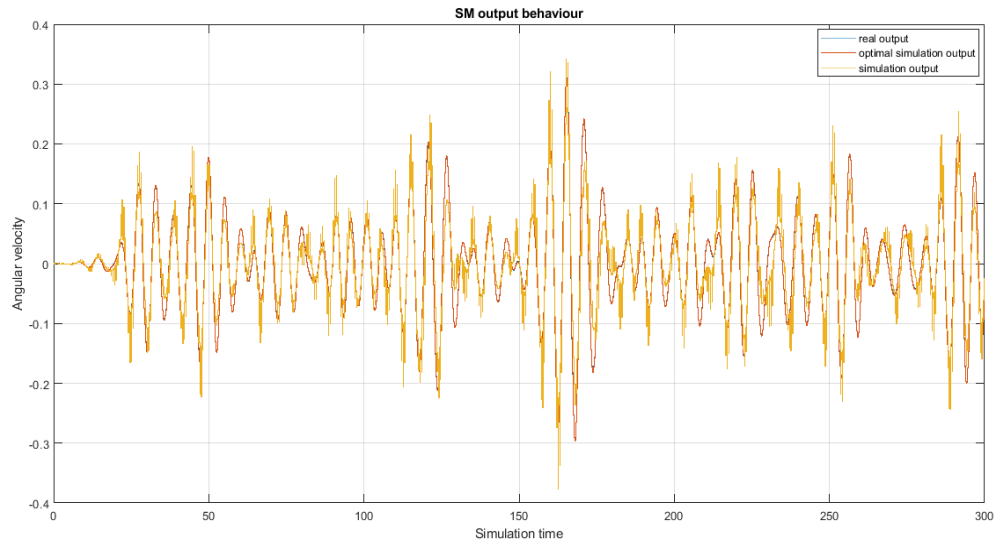


Figure 2.9: *Wave 3 tracking result.*

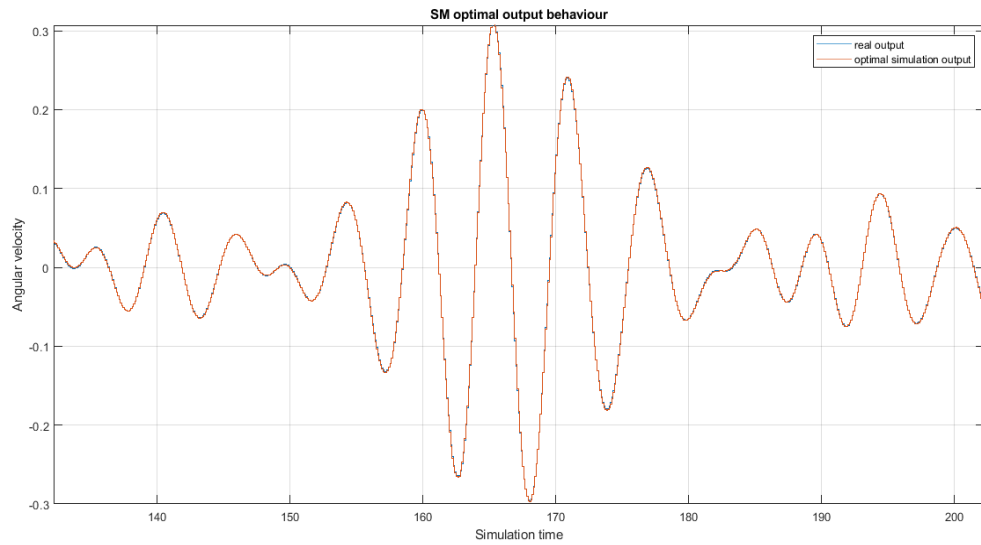


Figure 2.10: *Wave 3 optimal tracking result.*

In the figure2.9 a huge difference can be seen between the simulated output and the optimal one, due to the irregularity that the first one shows. More accurate is the optimal solution, that follows the reference in each point, as can be seen in detail in the figure 2.10.

The identification results for the 4th wave are shown in the following figure:

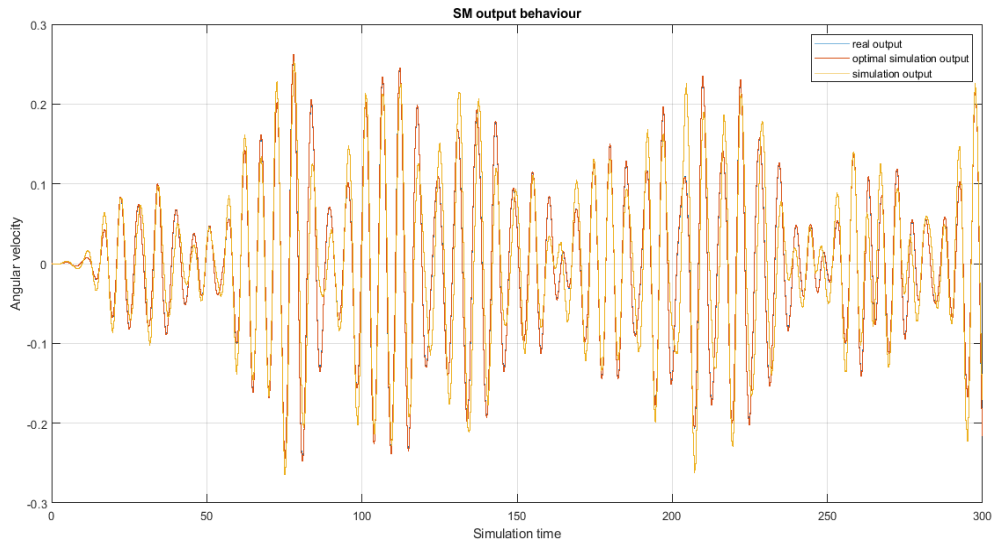


Figure 2.11: *Wave 4 tracking result.*

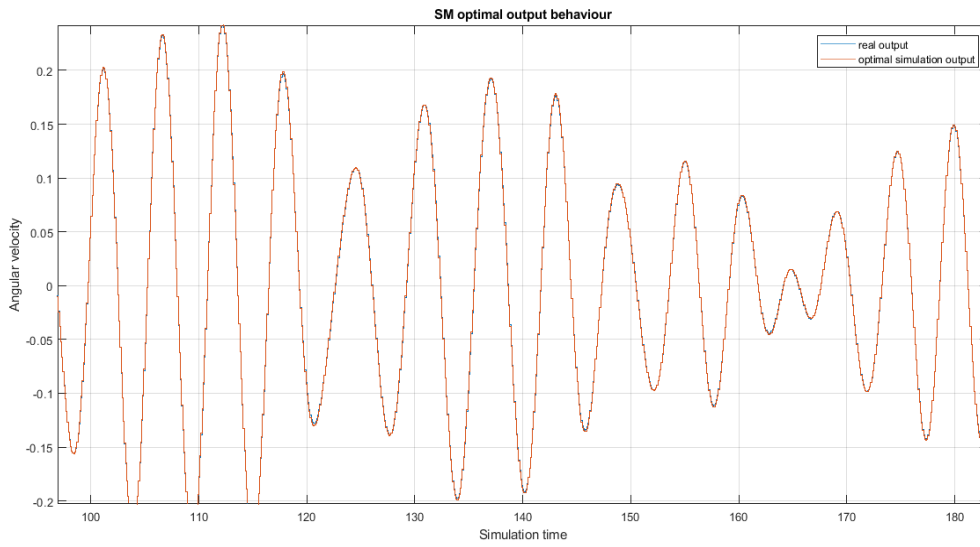


Figure 2.12: *Wave 4 optimal tracking result.*

As can be seen in the figures 2.11 and 2.12, the optimal solution is more efficient than the non-optimal. The same consideration can be done for each identification result.

The tracking result for wave 7 are the following:

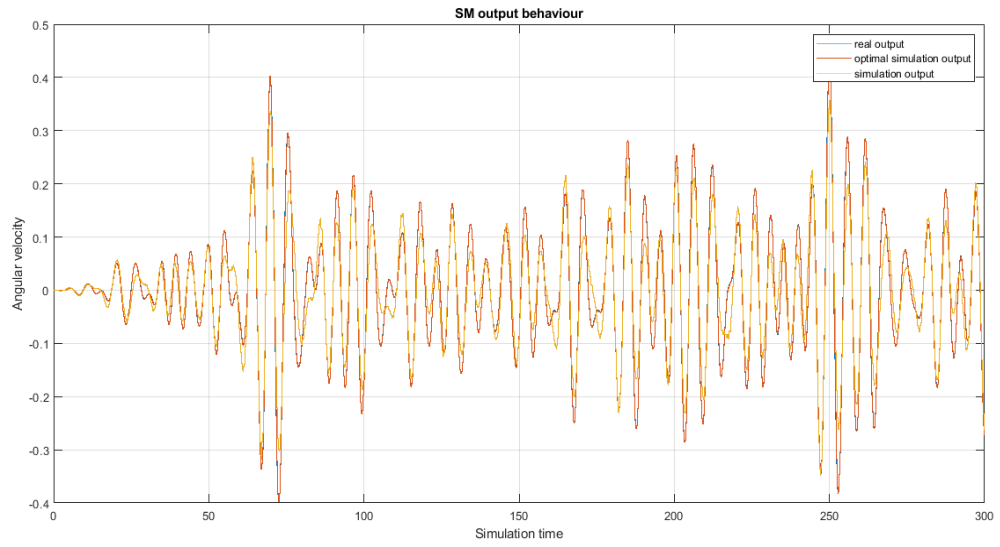


Figure 2.13: *Wave 7 tracking result.*

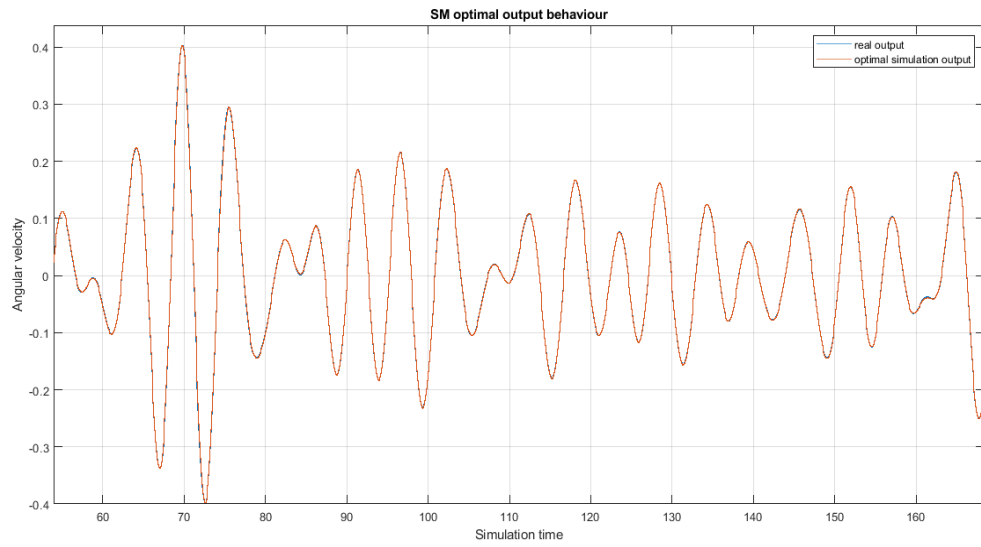


Figure 2.14: *Wave 7 optimal tracking result.*

The last identification result is for wave profile 9:

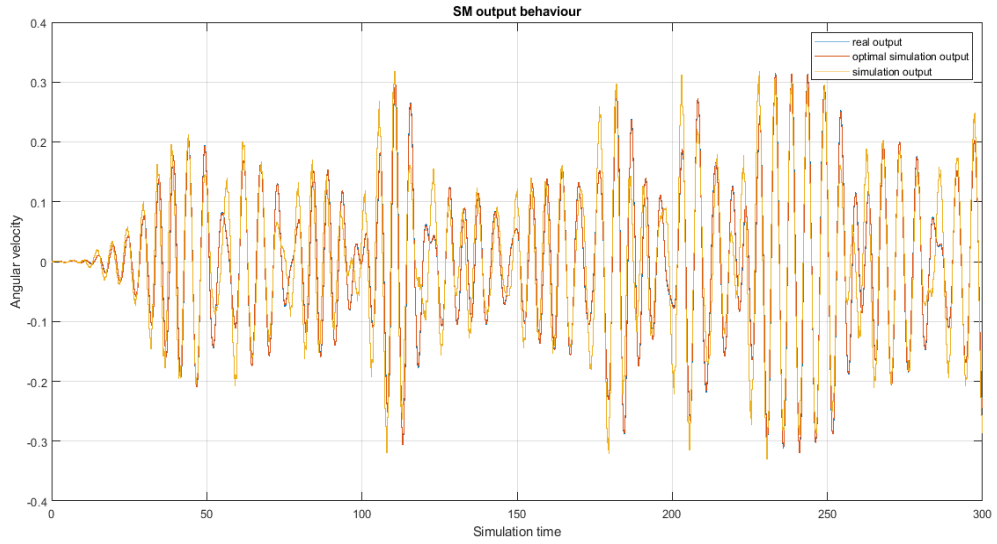


Figure 2.15: *Wave 9 tracking result.*

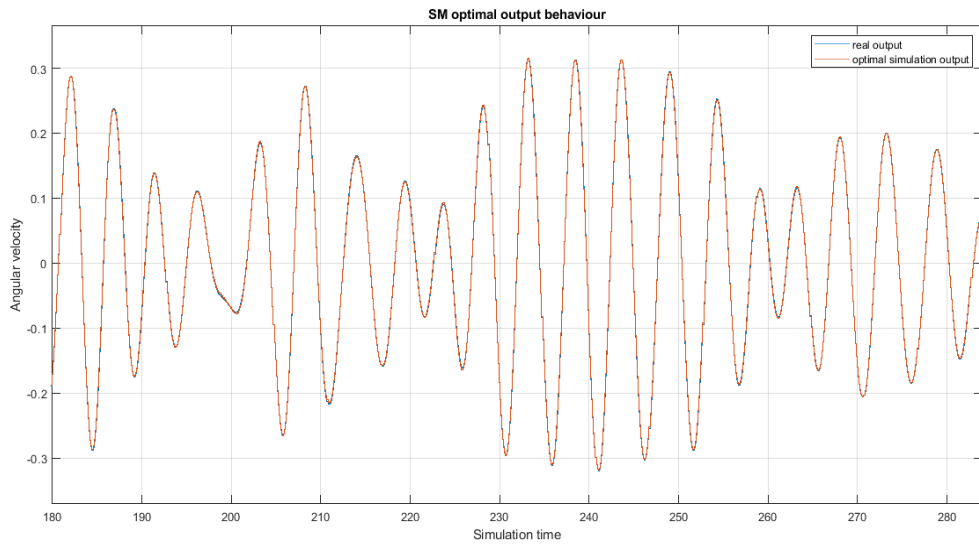


Figure 2.16: *Wave 9 optimal tracking result.*

The results used to find a controller through the H-inf approach are the optimal ones, in order to better represent the plant and the disturbance transfer functions.

The corresponding transfer functions, in the Laplace domain, are the following:

$$\begin{aligned}
 Gp3 &= \frac{-2.053 \cdot 10^{-5}s^3 - 0.0007286s^2 + 0.08548s - 0.148}{s^3 + 78.35s^2 + 3027s + 4.062 \cdot 10^4}; \\
 Gd3 &= \frac{8.286 \cdot 10^{-8}s^3 + 1.162 \cdot 10^{-6}s^2 + 1.447 \cdot 10^{-5}s + 7.987 \cdot 10^{-7}}{s^3 + 23.08s^2 + 1148s + 3307}; \\
 Gp4 &= \frac{-5.709 \cdot 10^{-6}s^3 - 0.0003014s^2 + 0.003925s - 0.1276}{s^3 + 75.32s^2 + 2870s + 3.707 \cdot 10^4}; \\
 Gd4 &= \frac{2.442 \cdot 10^{-8}s^3 + 6.777 \cdot 10^{-7}s^2 + 1.766 \cdot 10^{-5}s + 4.786 \cdot 10^{-5}}{s^3 + 38.54s^2 + 1481s + 1.338 \cdot 10^4}; \\
 Gp7 &= \frac{-7.984 \cdot 10^{-6}s^2 + 0.0007383s - 0.003009}{s^2 + 45.26s + 875.3}; \\
 Gd7 &= \frac{3.105 \cdot 10^{-8}s^3 + 5.047 \cdot 10^{-7}s^2 + 2.456 \cdot 10^{-6}s - 4.69 \cdot 10^{-6}}{s^3 + 26.16s^2 + 1211s + 7053}; \\
 Gp9 &= \frac{-9.037 \cdot 10^{-6}s^2 + 0.0001723s - 0.001413}{s^2 + 26.96s + 413.4}; \\
 Gd9 &= \frac{3.903 \cdot 10^{-8}s^3 + 7.264 \cdot 10^{-7}s^2 + 1.426 \cdot 10^{-5}s - 6.663 \cdot 10^{-5}}{s^3 + 30.22s^2 + 1291s + 1.184 \cdot 10^4}
 \end{aligned} \tag{2.25}$$

## 2.2.3 High order model identification

As in the previous section, the steps necessary in the identification are the same, but with an higher computational complexity due to the higher system degree.

### 2.2.3.1 Identification

Considering nine states, the plant transfer function and the disturbance transfer function are :

$$G_1(q^{-1}) = \frac{\dot{\varepsilon}_1(t)}{T_\varepsilon(t)} = \frac{\beta_{10} + \beta_{11}q^{-1} + \beta_{12}q^{-2} + \beta_{13}q^{-3} + \dots + \beta_{19}q^{-9}}{1 + \alpha_{11}q^{-1} + \alpha_{12}q^{-2} + \alpha_{13}q^{-3} + \dots + \alpha_{19}q^{-9}} \tag{2.26}$$

$$G_2(q^{-1}) = \frac{\dot{\varepsilon}_2(t)}{F_{ry}(t)} = \frac{\beta_{20} + \beta_{21}q^{-1} + \beta_{22}q^{-2} + \beta_{23}q^{-3} + \dots + \beta_{29}q^{-9}}{1 + \alpha_{21}q^{-1} + \alpha_{22}q^{-2} + \alpha_{23}q^{-3} + \dots + \alpha_{29}q^{-9}} \tag{2.27}$$

From the 2.26 and 2.27 it is possible to define the equality constraints of the problem:

$$\begin{aligned}
 \dot{\varepsilon}_1(t)(1 + \alpha_{11}q^{-1} + \alpha_{12}q^{-2} + \dots + \alpha_{19}q^{-9}) &= T_\varepsilon(t)(\beta_{10} + \beta_{11}q^{-1} + \beta_{12}q^{-2} + \dots + \beta_{19}q^{-9}) \\
 \dot{\varepsilon}_1(t) + \alpha_{11}\dot{\varepsilon}_1(t-1) + \dots + \alpha_{19}\dot{\varepsilon}_1(t-9) &= \beta_{10}T_\varepsilon(t) + \beta_{11}T_\varepsilon(t-1) + \dots + \beta_{19}T_\varepsilon(t-9) \\
 \dot{\varepsilon}_1(t) + \alpha_{11}\dot{\varepsilon}_1(t-1) + \dots + \alpha_{19}\dot{\varepsilon}_1(t-9) - \beta_{10}T_\varepsilon(t) - \beta_{11}T_\varepsilon(t-1) - \dots - \beta_{19}T_\varepsilon(t-9) &= 0
 \end{aligned} \tag{2.28}$$

The equation 2.28 is the first system equation. Following the same procedure for the disturbance transfer function, the result is:

$$\begin{aligned}\dot{\varepsilon}_2(t)(1 + \alpha_{21}q^{-1} + \alpha_{22}q^{-2} + \dots + \alpha_{29}q^{-9}) &= F_{ry}(\beta_{20} + \beta_{21}q^{-1} + \beta_{22}q^{-2} + \dots + \beta_{29}q^{-9}) \\ \dot{\varepsilon}_2(t) + \alpha_{21}\dot{\varepsilon}_2(t-1) + \dots + \alpha_{29}\dot{\varepsilon}_2(t-9) &= \beta_{20}F_{ry}(t) + \beta_{21}F_{ry}(t-1) + \dots + \beta_{29}F_{ry}(t-9) \\ \dot{\varepsilon}_2(t) + \alpha_{21}\dot{\varepsilon}_2(t-1) + \dots + \alpha_{29}\dot{\varepsilon}_2(t-9) - \beta_{20}F_{ry}(t) - \dots - \beta_{29}F_{ry}(t-9) &= 0\end{aligned}\quad (2.29)$$

The equation 2.29 is the second system equation. Considering the equations 2.28, 2.29, 2.17 and 2.12, it is possible to proceed to the *extended feasible parameter set (EFPS)*:

$$\begin{aligned}D_{\theta, \varepsilon_1, \varepsilon_2, \Delta\eta} &= \{\theta = [\alpha_{11}, \alpha_{12}, \dots, \alpha_{19}, \alpha_{21}, \alpha_{22}, \dots, \alpha_{29}, \\ &\quad \beta_{10}, \beta_{11}, \beta_{12}, \dots, \beta_{19}, \beta_{20}, \beta_{21}, \beta_{22}, \dots, \beta_{29}] \in \mathbb{R}^{38}, \\ &\quad \varepsilon_1 \in \mathbb{R}^N, \varepsilon_2 \in \mathbb{R}^N, \Delta\eta \in \mathbb{R}^1 : \\ \varepsilon_1(t) + \alpha_{11}\varepsilon_1(t-1) + \dots + \alpha_{19}\varepsilon_1(t-9) - \beta_{10}T_\varepsilon(t) - \beta_{11}T_\varepsilon(t-1) - \dots - \beta_{19}T_\varepsilon(t-9) &= 0 \\ \varepsilon_2(t) + \alpha_{21}\varepsilon_2(t-1) + \dots + \alpha_{29}\varepsilon_2(t-9) - \beta_{20}F_{ry}(t) - \dots - \beta_{29}F_{ry}(t-9) &= 0 \\ y(t) = \varepsilon_1(t) + \varepsilon_2(t) + \eta(t) \quad \rightarrow \quad \eta(t) = y(t) - \varepsilon_1(t) - \varepsilon_2(t) &\quad (2.30) \\ |\eta(t)| \leq \Delta\eta &\quad (2.31)\end{aligned}$$

Substituting the equation 2.30 into equation 2.31 and evolving the inequality, it is possible to obtain:

$$\begin{aligned}D_{\theta, \varepsilon_1, \varepsilon_2, \Delta\eta} &= \{\theta = [\alpha_{11}, \alpha_{12}, \dots, \alpha_{19}, \alpha_{21}, \alpha_{22}, \dots, \alpha_{29}, \\ &\quad \beta_{10}, \beta_{11}, \beta_{12}, \dots, \beta_{19}, \beta_{20}, \beta_{21}, \beta_{22}, \dots, \beta_{29}] \in \mathbb{R}^{38}, \\ &\quad \varepsilon_1 \in \mathbb{R}^N, \varepsilon_2 \in \mathbb{R}^N, \Delta\eta \in \mathbb{R}^1 : \\ \varepsilon_1(t) + \alpha_{11}\varepsilon_1(t-1) + \dots + \alpha_{19}\varepsilon_1(t-9) - \beta_{10}T_\varepsilon(t) - \dots - \beta_{19}T_\varepsilon(t-9) &= 0 \quad (2.32) \\ \varepsilon_2(t) + \alpha_{21}\varepsilon_2(t-1) + \dots + \alpha_{29}\varepsilon_2(t-9) - \beta_{20}F_{ry}(t) - \dots - \beta_{29}F_{ry}(t-9) &= 0 \quad (2.33) \\ y(t) - \varepsilon_1(t) - \varepsilon_2(t) \leq \Delta\eta \quad \rightarrow \quad \Delta\eta - y(t) + \varepsilon_1(t) + \varepsilon_2(t) \geq 0, \quad \forall t = 1, \dots, N &\quad (2.34) \\ -y(t) + \varepsilon_1(t) + \varepsilon_2(t) \leq \Delta\eta \quad \rightarrow \quad \Delta\eta + y(t) - \varepsilon_1(t) - \varepsilon_2(t) \geq 0, \quad \forall t = 1, \dots, N &\quad (2.35)\end{aligned}$$

The previous table shows the two equality constraints (2.32, 2.33) and the two inequality constraints 2.34, 2.35, so it is possible now to proceed to the the SparsePOP execution in order to solve the problem.

The objective function, in that case, is to minimize the error  $\Delta\eta$  and to find the respective parameter values.

The first step is to define the **objPoly**:

```
objPoly.typeCone = 1;
poly.degree = 1;
objPoly.dimVar = 39 + 2N;
objPoly.noTerms = 1;
```

```
objPoly.supports= zeros(1,39+2N)
objPoly.supports(1,39)= 1
objPoly.coef= 1;
```

The highest equation degree is 2, so the parameter  $tmin$  is 10. As for lower identification in previous section, the number of samples considered in the final simulation is 100, upon the total 3001 samples of each data. The first equality constraint is analyzed as follows:

$$\dot{\varepsilon}_1(t) + \alpha_{11}\dot{\varepsilon}_1(t-1) + \dots + \alpha_{19}\dot{\varepsilon}_1(t-9) - \beta_{10}T_\varepsilon(t) - \beta_{11}T_\varepsilon(t-1) - \dots - \beta_{19}T_\varepsilon(t-9) = 0$$

```
ineqPolySys{t-tmin+1}.typeCone=-1;
ineqPolySys{t-tmin+1}.degree= 2;
ineqPolySys{t-tmin+1}.dimVar=39+2N;
ineqPolySys{t-tmin+1}.noTerms=20;
ineqPolySys{t-tmin+1}.supports=A;
A=zeros(20, 39+2N); A(1,39+t)=1; A(2,1)=1; A(2,39+t-1)=1; A(3,2)=1;
  A(3,39+t-2)=1; A(4,3)=1; A(4,39+t-3)=1; A(5,4)=1; A(5,39+t-4)=1;
  A(6,5)=1; A(6,39+t-5)=1;
  A(7,6)=1; A(7,39+t-6)=1; A(8,7)=1; A(8,39+t-7)=1; A(9,8)=1; A(9,39+t-
    8)=1; A(10,9)=1; A(10,39+t-9)=1; A(11,10)=1; A(12,11)=1; A(13,12)=1;
  A(14,13)=1; A(15,14)=1; A(16,15)=1; A(17,16)=1; A(18,17)=1; A(19,18)=1;
  A(20,19)=1;
ineqPolySys{t-tmin+1}.coef=[ones(1,10) - T(t) ... - T(t-9)]';
```

The second equality constraint is analyzed as follows:

$$\dot{\varepsilon}_2(t) + \alpha_{21}\dot{\varepsilon}_2(t-1) + \dots + \alpha_{29}\dot{\varepsilon}_2(t-9) - \beta_{20}F_{ry}(t) - \beta_{21}F_{ry}(t-1) - \dots - \beta_{29}F_{ry}(t-9) = 0$$

```
ineqPolySys{t-2tmin+N+2}.typeCone=-1;
ineqPolySys{t-2tmin+N+2}.degree= 2;
ineqPolySys{t-2tmin+N+2}.dimVar=39+2N;
ineqPolySys{t-2tmin+N+2}.noTerms=20;
ineqPolySys{t-2tmin+N+2}.supports=B;
B=zeros(20, 39+2*N); B(1,39+N+t)=1; B(2,20)=1; B(2,39+N+t-1)=1;
  B(3,21)=1; B(3,39+N+t-2)=1; B(4,22)=1; B(4,39+N+t-3)=1; B(5,23)=1;
  B(5,39+N+t-4)=1;
  B(6,24)=1; B(6,39+N+t-5)=1; B(7,25)=1; B(7,39+N+t-6)=1; B(8,26)=1;
  B(8,39+N+t-7)=1; B(9,27)=1; B(9,39+N+t-8)=1;
  B(10,28)=1; B(10,39+N+t-9)=1; B(11,29)=1; B(12,30)=1; B(13,31)=1;
  B(14,32)=1; B(15,33)=1; B(16,34)=1; B(17,35)=1; B(18,36)=1; B(19,37)=1;
  B(20,38)=1;
ineqPolySys{t-2tmin+N+2}.coef=[ones(1,10) - F(t) ... - F(t-9)]';
```

The first inequality constraint is analyzed as follows:

$$\Delta\eta - y(t) + \dot{\varepsilon}_1(t) + \dot{\varepsilon}_2(t) \geq 0$$



```

ineqPolySys{t-3*tmin+2*N+3}.typeCone=1;
ineqPolySys{t-3*tmin+2*N+3}.degree= 1;
ineqPolySys{t-3*tmin+2*N+3}.dimVar=39+2N;
ineqPolySys{t-3*tmin+2*N+3}.noTerms=4;
ineqPolySys{t-3*tmin+2*N+3}.supports=C;
C=zeros(4, 39+2N); C(1,39+t)=1; C(2,39+N+t)=1; C(4,39)=1;
ineqPolySys{t-3*tmin+2*N+3}.coef=[1 1 -y(t) 1]';

```

The second inequality constraint is analyzed as follow:

$$\Delta\eta + y(t) - \varepsilon_1(t) - \varepsilon_2(t) \geq 0$$

```

ineqPolySys{t-4*tmin+3*N+4}.typeCone=1;
ineqPolySys{t-4*tmin+3*N+4}.degree= 1;
ineqPolySys{t-4*tmin+3*N+4}.dimVar=39+2N;
ineqPolySys{t-4*tmin+3*N+4}.noTerms=4;
ineqPolySys{t-4*tmin+3*N+4}.supports=D;
D=zeros(4, 39+2N); D(1,39+t)=1; D(2,39+N+t)=1; D(4,39)=1;
ineqPolySys{t-4*tmin+3*N+4}.coef=[-1 -1 y(t) 1]';

```

The support matrix is the same of first inequality constraint.

The lower bound and upper bound are considered as following:

$$\begin{aligned}
lbd &= [-1e10ones(1,39+2N)]; \\
ubd &= [1e10ones(1,39+2N)];
\end{aligned}$$

Also here the param.relaxOrder is 1 and the param.POPsolver is set to "active-set". In order to find the minimum error  $\Delta\eta$ (objective function) and the associated parameter values,the following code is used:

```

[~,~,POP]=sparsePOP(objPoly,ineqPolySys,lbd,ubd,param);
delta_eta = POP.xVect(39);
for j=1:38
    th(j)=POP.xVect(j);
end
delta_etaL = POP.xVectL(39);
for j=1:38
    thL(j)=POP.xVectL(j);
end

```

where "L" indicates the parameters found as optimal solution. The plant and disturbance transfer functions, corresponding to the non-optimal solution and optimal

solution, are found considering the Z-domain transfer functions:

$$\begin{aligned}
 Gp_{-z} &= \frac{th(10)z^9 + th(11)z^8 + th(12)z^7 + \dots + th(18)z + th(19)}{z^9 + th(1)z^8 + th(2)z^7 + \dots + th(8)z + th(9)} \\
 Gd_{-z} &= \frac{th(29)z^9 + th(30)z^8 + \dots + th(37)z + th(38)}{z^9 + th(20)z^8 + th(21)z^7 + \dots + th(27)z + th(28)} \\
 Gp_{-z-L} &= \frac{thL(10)z^9 + thL(11)z^8 + thL(12)z^7 + \dots + thL(18)z + thL(19)}{z^9 + thL(1)z^8 + thL(2)z^7 + \dots + thL(8)z + thL(9)} \\
 Gd_{-z-L} &= \frac{thL(29)z^9 + thL(30)z^8 + thL(31)z^7 + \dots + thL(37)z + thL(38)}{z^9 + thL(20)z^8 + thL(21)z^7 + \dots + thL(27)z + thL(28)}
 \end{aligned} \tag{2.36}$$

### 2.2.3.2 Identification results

As the two degree identification, the better results are found using the "active-set", obtaining the optimal solution and the reference tracking result are very similar to the two degree ones.

## Chapter 3

# Robust Control

In this chapter are introduced the main theory knowledge of Robust Control and the two cases analyzed (second degree and ninth degree). After that, the next step is to simulate the non linear model (MPC Simulink scheme) with the two Robust controllers, substituting the MPC proper one. The interested readers can find details about Robust control in the following books [11] and [12].

### 3.1 Basic notions

Robustness of a control system is the capability of a feedback system to keep its properties with respect to disturbances and uncertainties. The considering feedback system in this approach, with the respective disturbance, is the following:

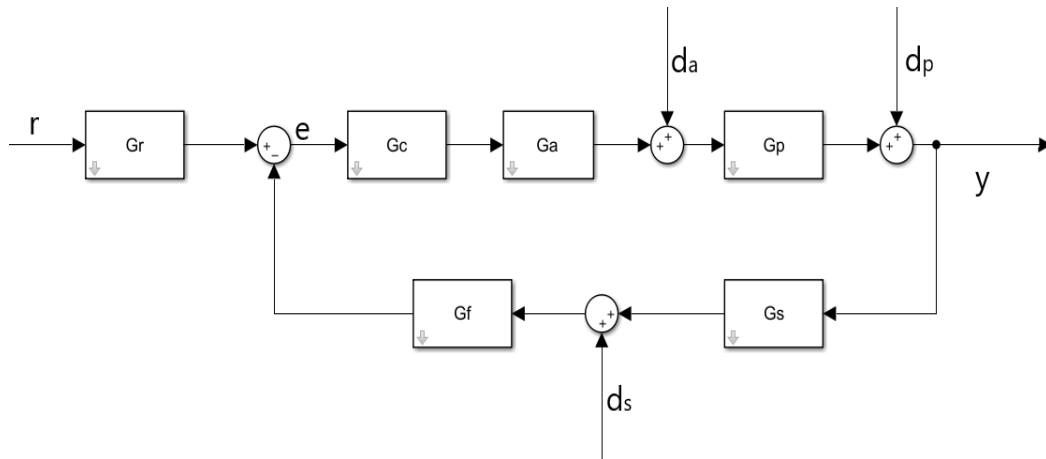


Figure 3.1: *Feedback system.*

with

- $r$ : reference;
- $e$ : error;

- $d_a$ : disturbance on actuator;
- $d_p$ : disturbance on plant;
- $d_s$ : disturbance on sensor;

The *loop function*  $L(s)$  is given by:

$$L(s) = G_c \cdot G_a \cdot G_p \cdot G_s \cdot G_f$$

In order to introduce some constraints with respect to the disturbances, the *sensitivity function*  $S(s)$  and *complementary sensitivity function*  $T(s)$  are considered:

$$S(s) = \frac{1}{1 + L(s)}; \quad T(s) = \frac{L(s)}{1 + L(s)};$$

It is possible to find some correlations between these three functions.

The typical behavior of the three functions can be represented in the following Bode diagram:

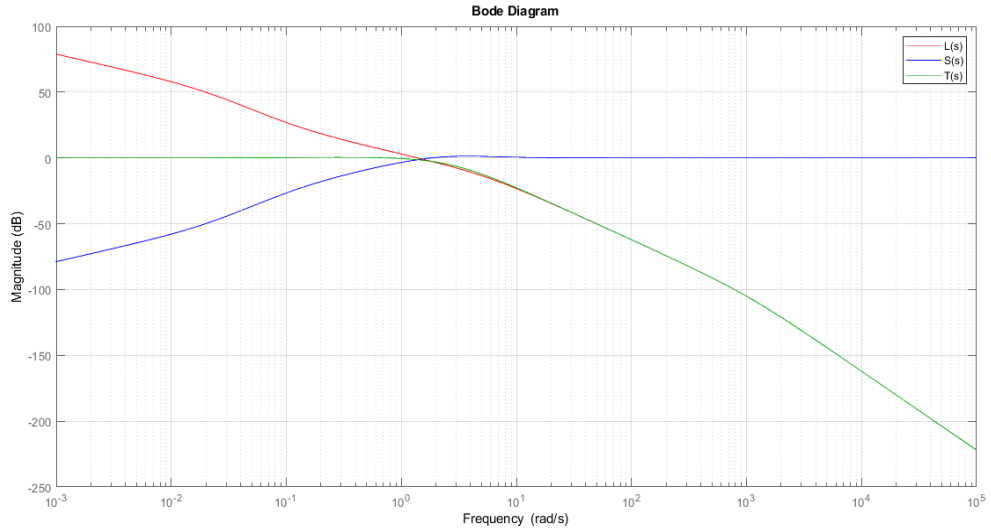


Figure 3.2: *Bode diagram.*

Assuming that the cutting frequency of the loop function on 0 dB axis is  $w_c$ , it is possible to subdivide the frequency behavior in 2 main classes:

- $w \ll w_c$ :  $|S(jw)| = \left| \frac{1}{1+L(jw)} \right| \approx \frac{1}{|L(jw)|}$ ;
- $w \gg w_c$ :  $|T(jw)| = \left| \frac{L(jw)}{1+L(jw)} \right| \approx |L(jw)|$ ;

In the performance study, it is possible to use the sensitivity function and the complementary sensitivity function in order to avoid a the disturbance noise in  $L(s)$ . Let's consider the case of a disturbance on the sensor as a sinusoidal disturbance.

$$d_s = a_s \sin(w_s t + \varphi_s)$$

The output error at steady-state, as request, has to be bounded by a constant.

$$|e_{d_s}^\infty| = |y_{d_s}^\infty| \leq \rho_s \quad \rho_s > 0$$

Considering the feedback system of figure 3.1 , from the error equation it is possible to approximate a mask on loop function:

$$\begin{aligned} |e_{d_s}^\infty| = |y_{d_s}^\infty| &= |a_s|T(jw_s)|\frac{1}{G_s}\sin(w_s t + \varphi_s)| \leq a_s|T(jw_s)|\frac{1}{G_s} \leq \rho_s \rightarrow \\ &\rightarrow |T(jw_s)| \leq \frac{\rho_s G_s}{a_s} \quad \forall w_s \geq w_s^- \end{aligned} \quad (3.1)$$

Considering that at the high frequencies the loop function and complementary sensitivity function are similar, it is possible to obtain the following constraint:

$$|e_{d_s}^\infty| \leq \rho_s \rightarrow L(jw_s) \leq \frac{\rho_s G_s}{a_s} = M_T^{HF} \quad (3.2)$$

A similar procedure can be found at low frequencies, for disturbance on plant, on the sensitivity function.

Taking in analysis a sinusoidal disturbance

$$d_p = a_p \sin(w_p t + \varphi_p)$$

bounded by a chosen constant

$$|e_{d_p}^\infty| = |y_{d_p}^\infty| \leq \rho_p \quad \rho_p > 0$$

As the previous case, considering that at very low frequencies the loop function frequency behavior can be approximated as the inverse of sensitivity function one, from the error equation is possible to obtain a low frequency mask:

$$\begin{aligned} |e_{d_p}^\infty| = |y_{d_p}^\infty| &= |a_p|S(jw_p)|\sin(w_p t + \varphi_p)| \leq a_p|S(jw_p)| \leq \rho_p \rightarrow \\ &\rightarrow |S(jw_p)| \leq \frac{\rho_p}{a_p} = M_S^{LF} \quad \forall w_p \leq w_p^+ \rightarrow \\ &\rightarrow L(jw_p) \geq \frac{a_p}{\rho_p} = \frac{1}{M_S^{LF}} \end{aligned} \quad (3.3)$$

The two equations 3.2 and 3.3 allow to take care of the disturbance contribution in the performance analysis phase.

In the following figure is shown an example of this analysis:

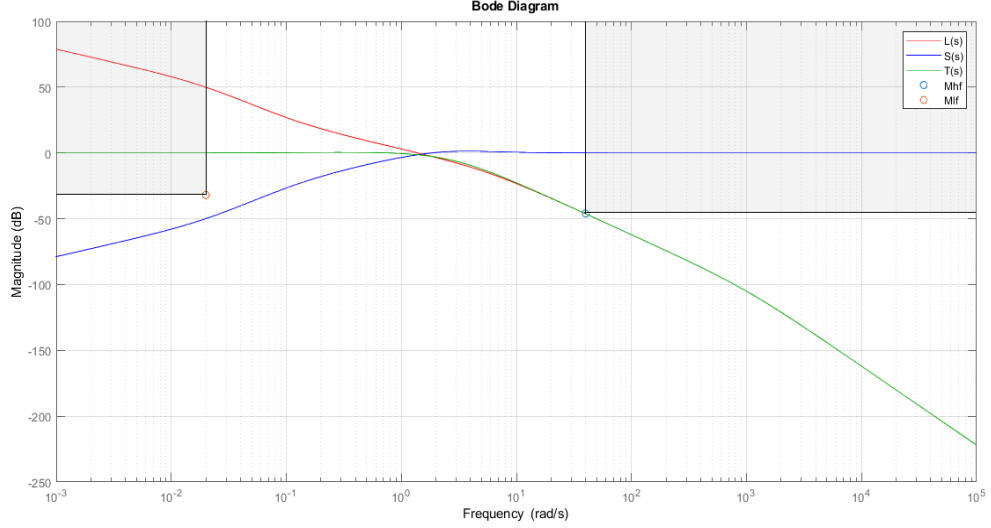


Figure 3.3: *Disturbance constraints.*

In order to have some masks on  $S(jw)$  and  $T(jw)$  which cover them from frequency domain constraints,  $W_S(jw)$  and  $W_T(jw)$  are considered. The constraints can be written in the following form:

$$|T(jw)| \leq |W_T^{-1}(jw)| \quad |S(jw)| \leq |W_S^{-1}(jw)| \quad \forall w \quad (3.4)$$

Translating those requirements in  $H_\infty$  norm, it is obtained:

$$\|W_T(s)T(s)\|_\infty \leq 1 \quad , \quad \|W_S(s)S(s)\|_\infty \leq 1$$

In order to construct the two masks  $W_T$  and  $W_S$ , the different constraints are obtained by the steady state requirements. From the equation 3.4, for a matter of simplicity the two masks are projected in the inverse way.

Taking in analysis a two degree form, the mask mathematical models are the following:

$$W_T^{-1} = \frac{T_{po}}{(1 + \frac{s}{p})^2}; \quad W_S^{-1} = \frac{as(1 + \frac{s}{w1})}{1 + 1.414\frac{s}{w2} + (\frac{s}{w2})^2} \quad (3.5)$$

- $T_{po}$  and  $S_{po}$  are the peaks, obtained by the choice of damping factor  $\zeta$ :

$$T_p \leq \frac{1}{2\zeta\sqrt{1-\zeta^2}} = T_{po} \quad ; \quad S_p \leq \frac{2\zeta\sqrt{2+4\zeta^2+2\sqrt{1+8\zeta^2}}}{\sqrt{1+8\zeta^2+4\zeta^2-1}} = S_{po} \quad (3.6)$$

- $M_T^{HF}$  and  $M_S^{LF}$  as described in equations 3.2 and 3.3;

- $\nu + p$  = number of zeros in origin of  $S(jw)$ , where  $\nu$  is the number of zeros in origin of the controller and  $p$  is the number of zeros in the origin of the plant;
- low frequency constraint for  $S$ :

$$\lim_{s \rightarrow 0} \frac{1}{s^{\nu+p}} W_S^{-1} = a; \quad (3.7)$$

- high frequency constraint for  $S$ :

$$\lim_{s \rightarrow \infty} W_S^{-1} = S_{po} = \frac{\frac{a}{w_1}}{\frac{1}{w_2^2}} \rightarrow w_2 = \sqrt{\frac{S_{po} w_1}{a}} \quad (3.8)$$

### 3.1.1 Model uncertainty

The model uncertainty characterizes the mathematical models, caused by physical approximated parameters known partially (parametric uncertainty) or by unmodeled dynamic (dynamic uncertainty). Concerning this, the *model set* is the set of system from which the chosen plant is taken.

It is possible to classify the model set in two main uncertainty model set:

- *structured model set*: set parametrized by a finite number of parameters;
- *unstructured model set*: the phase behavior and the order of the system are unknown;

Taking into consideration the unstructured uncertainty model set and considering the following notations

- $G_p(s)$ : transfer function of the generic member of the uncertainty model set;
- $G_{pn}(s)$ : transfer function of *nominal model*;
- $\Delta(s)$ : any transfer function with an  $H_\infty$  norm less than 1;
- $W_u$ : weighting function that takes into account the uncertainty;

can be highlighted four approaches:

1. *Additive uncertainty*:  $M_a = \{G_p(s) : G_p(s) = G_{pn}(s) + W_u(s)\Delta(s), \|\Delta(s)\|_\infty \leq 1\}$
2. *Multiplicative uncertainty*:  $M_m = \{G_p(s) : G_p(s) = G_{pn}(s) [1 + W_u(s)\Delta(s)], \|\Delta(s)\|_\infty \leq 1\}$
3. *Inverse additive uncertainty*:  $M_{ia} = \left\{G_p(s) : G_p(s) = \frac{G_{pn}(s)}{1 + W_u(s)\Delta(s)}, \|\Delta(s)\|_\infty \leq 1\right\}$
4. *Inverse multiplicative uncertainty*:  $M_{im} = \left\{G_p(s) : G_p(s) = \frac{G_{pn}(s)}{1 + W_u(s)\Delta(s)}, \|\Delta(s)\|_\infty \leq 1\right\}$

In the thesis work the used approaches are the additive uncertainty and the multiplicative uncertainty. The previous equations give some kind of constraints, based on the weighted function  $W_u$ .

Considering the additive uncertainty case, the model set is:

$$\begin{aligned} M_a &= \{G_p(s) : G_p(s) = G_{pn}(s) + W_u(s)\Delta(s), \|\Delta(s)\|_\infty \leq 1\} \rightarrow \\ &\rightarrow \left\| \frac{G_p(s) - G_{pn}(s)}{W_u(s)} \right\|_\infty = \|\Delta(s)\|_\infty \leq 1 \rightarrow |G_p(jw) - G_{pn}(jw)| \leq |W_u(jw)| \quad \forall w \end{aligned} \quad (3.9)$$

In a similar way, examining the multiplicative uncertainty model set:

$$\begin{aligned} M_m &= \{G_p(s) : G_p(s) = G_{pn}(s) [1 + W_u(s)\Delta(s)], \|\Delta(s)\|_\infty \leq 1\} \rightarrow \\ &\rightarrow \left\| \left( \frac{G_p(s)}{G_{pn}(s)} - 1 \right) \frac{1}{W_u(s)} \right\|_\infty = \|\Delta(s)\|_\infty \leq 1 \rightarrow \left| \frac{G_p(jw)}{G_{pn}(jw)} - 1 \right| \leq |W_u(jw)| \quad \forall w \end{aligned} \quad (3.10)$$

The equations 3.9 and 3.10 can be interpreted as the presence of a mask that covers the general relation between the set of plant and the nominal one. For example, considering the multiplicative set case, the Bode result is the following:

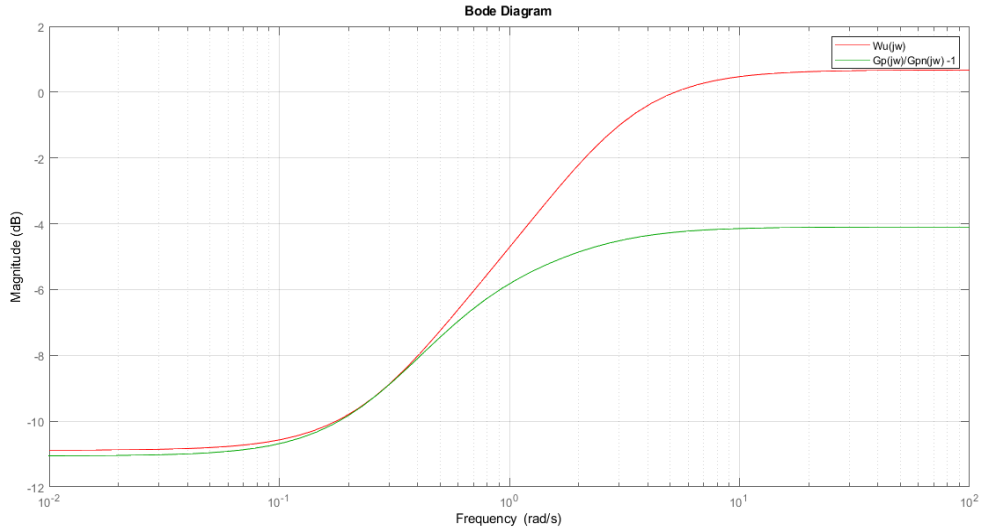
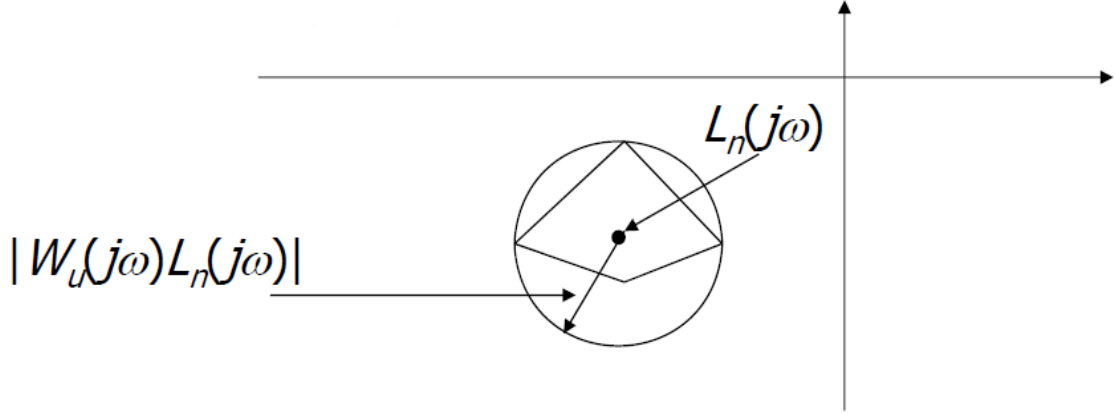


Figure 3.4: *Multiplicative uncertainty model.*

From now on, due to the thesis purpose, the attention is focused to the multiplicative uncertainty model.

The eq.3.10 gives a not exactly description of parametric uncertainties, but a conservative one. In particular, being the complex function  $\Delta(s)$  a real number, the uncertainty is represented as a disk of radius  $|W_u(jw)L_n(jw)|$  at each frequency  $w$ , as shown in figure 3.5:




 Figure 3.5: *Conservative uncertainty model.*

The condition of *Robust Stability* is achieved if:

$$\|W_u T_n\|_\infty < 1 \quad (3.11)$$

only if the following assumptions are satisfied:

- $G_p$  belongs to the multiplicative uncertainty model set  $M_m$ ;
- considering  $G_{pn}$  as nominal model of the plant, the feedback system is stable;

The condition of *Nominal Performance* for sensitivity function and complementary sensitivity function is achieved if:

$$\|W_S S_n\|_\infty < 1 \quad , \quad \|W_T T_n\|_\infty < 1 \quad (3.12)$$

The *Robust Performance* condition for a feedback system is:

$$\| |W_S S_n| + |W_T T_n| \|_\infty < 1 \quad (3.13)$$

### 3.1.2 Robust control through $H_\infty$

The  $H_\infty$  norm of a SISO LTI system  $H(s)$  is defined as:

$$\|H(s)\|_\infty = \max_{\omega} |H(j\omega)| \quad (3.14)$$

The  $H_\infty$  control ( $H_\infty$  norm minimization approach), considers as feedback system the following diagram:

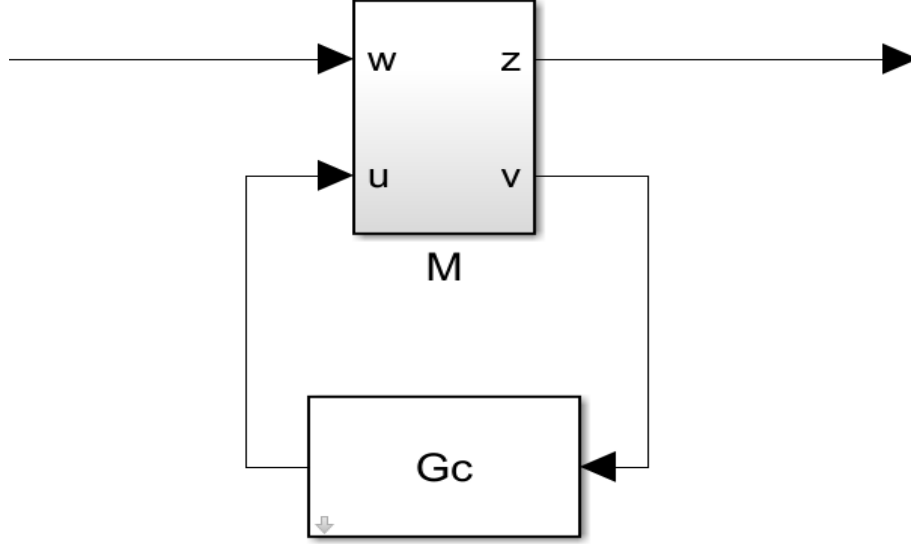


Figure 3.6: *Generalized plant model.*

- $M$ : generalized plant;
- $G_c$ : controller;
- $w$ : external inputs;
- $u$ : control inputs;
- $z$ : external outputs;
- $v$ : controller inputs;

Considering  $G_c^{stab}$  as the set of controllers that guarantees internal stability to nominal feedback system, and  $T_{wz}$  as the closed loop transfer function between  $w$  and  $z$ , the controller is obtained optimizing the following equation:

$$G_c(s) = \arg \min_{G_c \in G_c^{stab}} \|T_{wz}\|_\infty \quad (3.15)$$

In order to find a controller that guarantees both conditions of Nominal Performance and Robust Stability, the  $H_\infty$  norm conditions to be satisfied are:

$$\|W_S S_n\|_\infty < 1 \quad , \quad \|W_T T_n\|_\infty < 1 \quad , \quad \|W_u T_n\|_\infty < 1$$

The function  $T_{wz}$  has to take into account the previous conditions, so it is considered as:

$$T_{wz}(s) = \begin{bmatrix} W_1 S_n \\ W_2 T_n \end{bmatrix} \quad (3.16)$$

with

$$W_1(s) = W_S(s) \quad , \quad |W_2(jw)| = \max(|W_u(jw)|, |W_T(jw)|)$$

Considering the equation 3.16 , the generalized plant model is:

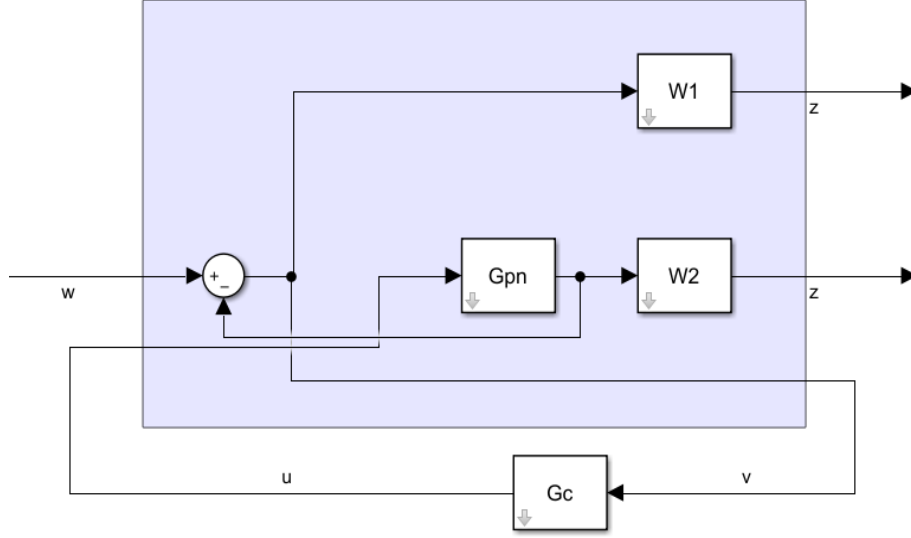


Figure 3.7: Total generalized plant model.

In order to solve the eq. 3.16 , the *LMI optimization approach (linear matrix inequalities)* is used. In order to have a generalized plant  $M$  that can be internally stabilized, the weighted functions  $W_1$  and  $W_2$  must be stable transfer functions. Due to the previous conditions, the transfer functions  $W_1$  and  $W_2$  have to be modified before to introduce them in the generalized plant. As far as it concerns the transfer function  $W_1 = W_S$ , the pole in the origin is a source of instability, so it is substituted by a very lower pole:

$$W_1^{mod}(s) = W_1 \frac{s^{v+p}}{(s + \lambda^*)^{v+p}} \quad (3.17)$$

where

$$\lambda^* \leq 0.01w_c$$

After obtaining the controller, the pole in  $s = -\lambda^*$  will be substituted by a pole in the origin. Concerning the transfer function  $W_2$ , it is not possible to introduce in Simulink an improper fraction, so the two zeros are introduced with the Matlab command "*sderiv*" and the  $W_2^{mod}$  becomes:

$$W_2^{mod} = \frac{1}{T_{po}} \quad (3.18)$$

## 3.2 Robust Control in ISWEC model

### 3.2.1 Low order model $H_\infty$ approach

In order to compute the controller, the plant and the disturbance transfer function of second degree found in the SM chapter are considered. The feedback system considered in this step is the following:

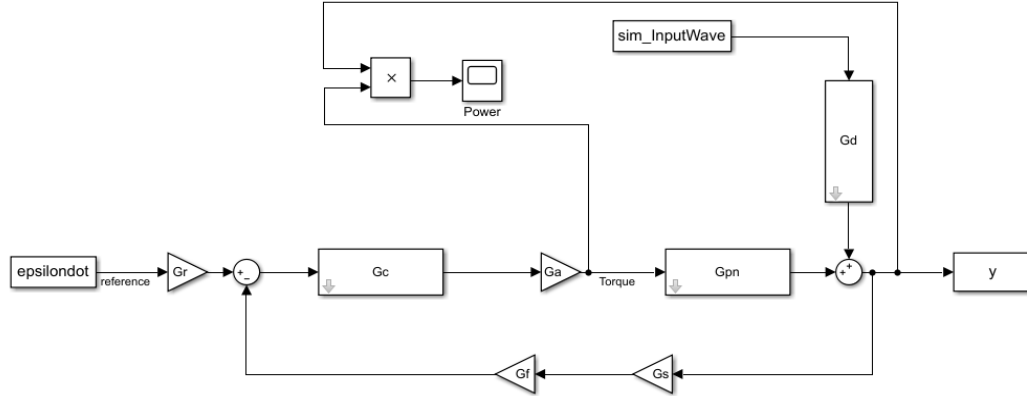


Figure 3.8:  $H_\infty$  feedback system.

The first step is to start from steady state requirements. In this phase, the different bounds are imposed in a preliminary way. It is possible to interpret the scheme of figure 3.8 with the following block schemes:

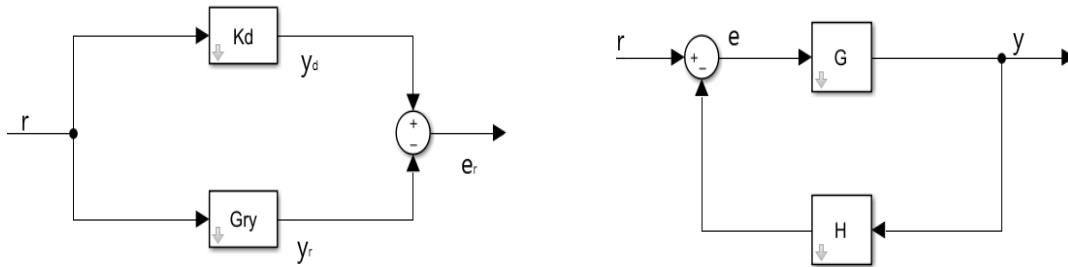


Figure 3.9:  $H_\infty$  Feedback block schemes.

- $K_d$ : desired steady state gain;
- $y_d$ : desired output;
- $G_{ry}$ : closed loop function;
- $y_r$ : real output;

- $e_r$ :error;

It is assumed that  $G_s = G_r = G_a = 1$ .

The desired steady-state gain of the feedback control system  $K_d$  is 1, so assuming that  $\nu + p \geq 1$ :

$$H = G_s G_f = \frac{1}{K_d} \rightarrow G_f = \frac{1}{G_s K_d} = 1; \quad (3.19)$$

The steady-state output error requirement is:

$$|e_r^\infty| < 0.03; \quad (3.20)$$

The reference  $r(t)$  and the plant disturbance  $d_p(t)$  are approximated to sinusoidal waves. The steady-state tracking error expression is:

$$e_r^\infty(t) = \rho R_0 \sin(w_0 t + \varphi) \quad (3.21)$$

where  $\rho$  is the max error value,  $R_0$  is the max reference value.

The value of  $\rho$  is:

$$\rho = \left| \frac{1}{1 + L(jw_0)} \right| = |S(jw_0)| \quad (3.22)$$

From equation 3.22 it is possible to understand that the bigger is  $w_0$ , the bigger is the error  $\rho$ . The desired transient time requirements are:

- Overshoot  $\hat{s} < 0.1$ ;
- Settling time  $t_{s,5\%} < 25s$ ;
- Rise time  $t_r < 3s$ ;

From these desired parameters it is possible to find some constraints for the project design:

- Damping factor  $\zeta \geq \frac{|\ln(\hat{s})|}{\sqrt{\pi^2 + \ln^2(\hat{s})}} = 0.59$ ;
- Complementary sensitivity function peak  $T_p = \frac{1}{2\zeta\sqrt{1-\zeta^2}} = 1.05 = T_{po}$ ;
- Sensitivity function peak  $S_p = \frac{2\zeta\sqrt{2+4\zeta^2+2\sqrt{1+8\zeta^2}}}{\sqrt{1+8\zeta^2+4\zeta^2-1}} = 1.3 = S_{po}$ ;
- cutting frequency  $\omega_c \geq \frac{1}{t_r} \frac{1}{\sqrt{1-\zeta^2}} (\pi - \arccos(\zeta)) \cdot \sqrt{\sqrt{1+4\zeta^4} - 2\zeta^2} = 0.23 \frac{rad}{s}$ ;  
 $\omega_c \geq \frac{\ln(0.05)}{\zeta} \sqrt{\sqrt{1+4\zeta^4} - 2\zeta^2} \frac{1}{t_{s,5\%}} = 0.18 \frac{rad}{s}$ ;

The successive step is the definition of  $W_T(s)$  and  $W_S(s)$ .

The sensitivity function is designed as:

$$W_S^{-1}(s) = \frac{as(1 + \frac{s}{w_1})}{1 + 1.414w_2 + (\frac{s}{w_2})^2} = \frac{0.1s(1 + \frac{s}{3})}{1 + 5.19 + (\frac{s}{3.67})^2} \quad (3.23)$$

where  $w_2 = \sqrt{\frac{w_1 S_{po}}{a}}$ .

The complementary sensitivity function is the following:

$$W_T^{-1}(s) = \frac{T_{po}}{1 + \frac{s}{p}} = \frac{1.05}{1 + \frac{s}{500}} \quad (3.24)$$

The following step is to define the uncertainty weighted function  $W_u$ .

The four plants of second order are considered. Considering multiplicative uncertainty, the following Matlab code is used in order to find the desired weighted function:

```
Gp=[G1p; G2p; G3p; G4p];
for i=1:4
    omega=logspace(-2,2,1000);
    delta_m=Gp(i)/Gp(2) -1;
    [m, f]=bode(delta_m,omega);
    mag=squeeze(m);
    loglog(omega,mag),grid on,
    hold on
end
mf=ginput(20);
magg=vpck(mf(:,2),mf(:,1));
Wu=fitmag(magg);
[A, B, C, D]=unpck(Wu);
[Z, P, K]=ss2zp(A,B,C,D);
Wu=minreal(zpk(Z,P,K),1e-3)
```

The final  $W_u$  considering as nominal plant the second plant(fourth wave profile) is:

$$W_u = \frac{3.0854(s + 0.2099)(s + 64.64)}{s^2 + 15.08s + 327.1} \quad (3.25)$$

In order to proceed to the  $H_\infty$  solution, the  $T_{wz}$  must be defined.

$$T_{wz}(s) = \begin{bmatrix} W_1 S_n \\ W_2 T_n \end{bmatrix}$$

$$W_1(s) = W_S(s) \quad , \quad |W_2(jw)| = \max(|W_u(jw)|, |W_T(jw)|)$$

To find  $W_2$ , the two Bode diagrams of  $W_T$  and  $W_u$  are analyzed:

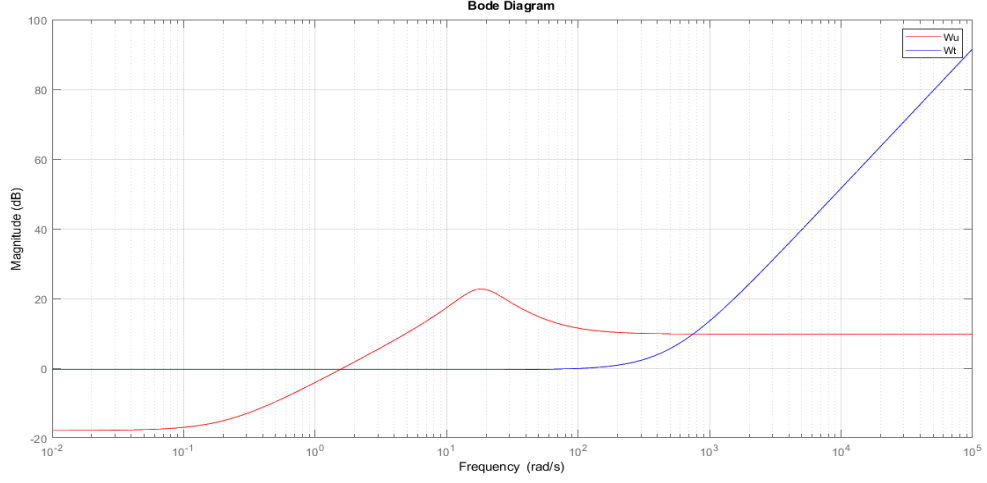


Figure 3.10: Bode diagram of  $W_T$  and  $W_u$ .

The two functions have a superposition, so as  $W_2$  is considered the mask  $W_T$ , because the function  $W_u$  is major only for a little interval. Substituting the  $W_1$  pole in origin with a pole in  $0.01w_c$  and doing some gain modifications also on  $W_2$ , the obtained controller through *lmi optimization* is the following:

$$G_c = \frac{-2.2439 \cdot 10^6 (s + 21.75)(s + 1.337)(s + 0.1)(s + 8.873 \cdot 10^4)(s + 1.187 \cdot 10^5)(s^2 + 53.57s + 1704)}{s(s + 6.471 \cdot 10^4)(s + 3039)(s + 173.3)(s + 0.1066)(s + 0.09258)(s^2 + 75.26s + 1.026 \cdot 10^4)} \quad (3.26)$$

The first analysis to do is the tracking of the reference, and the correct production of power.

The tracking of reference is the following:

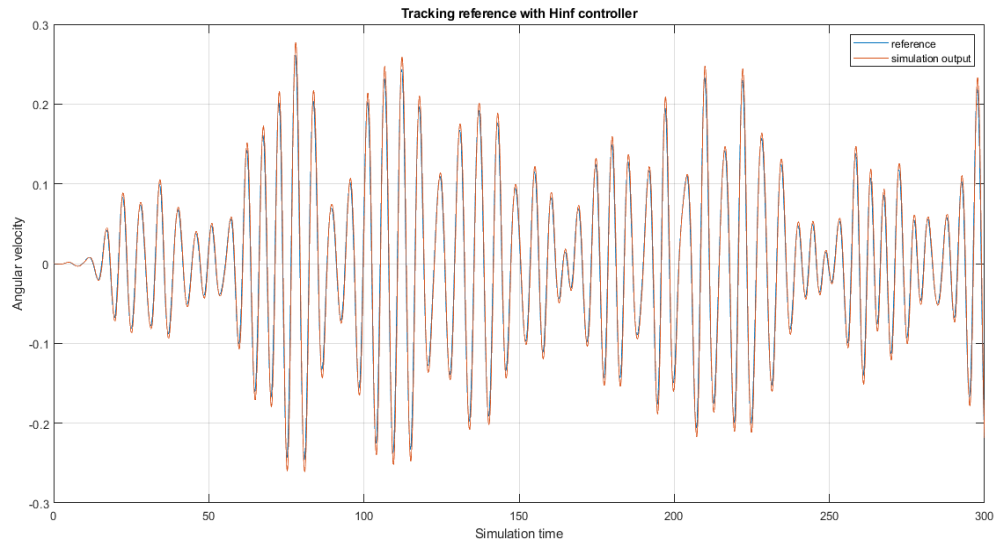


Figure 3.11: *Tracking of the reference with low order controller.*

The simulation output follows in a good way the reference, with an error margin of about 0.02.

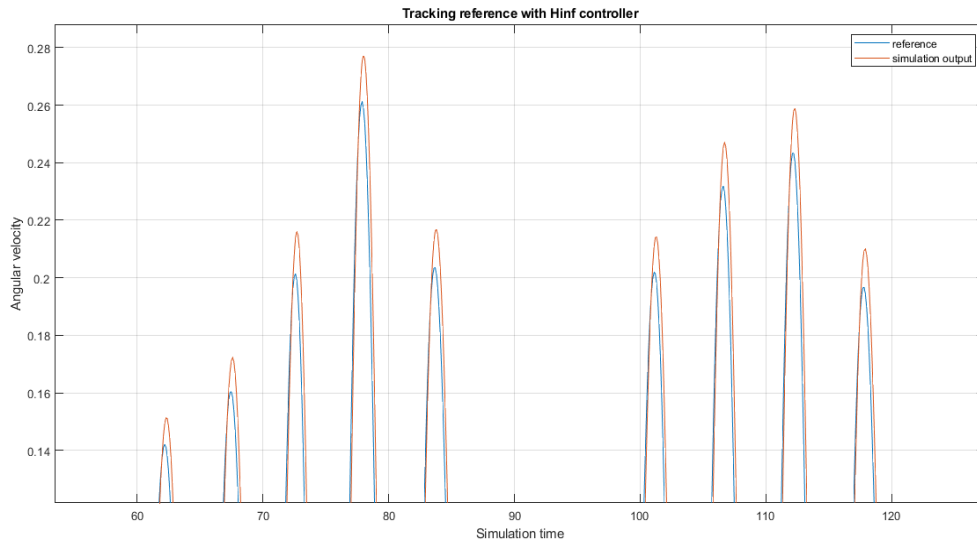


Figure 3.12: *Tracking error of the reference with low order controller.*



The comparison between the MPC torque and the Robust one is the following:

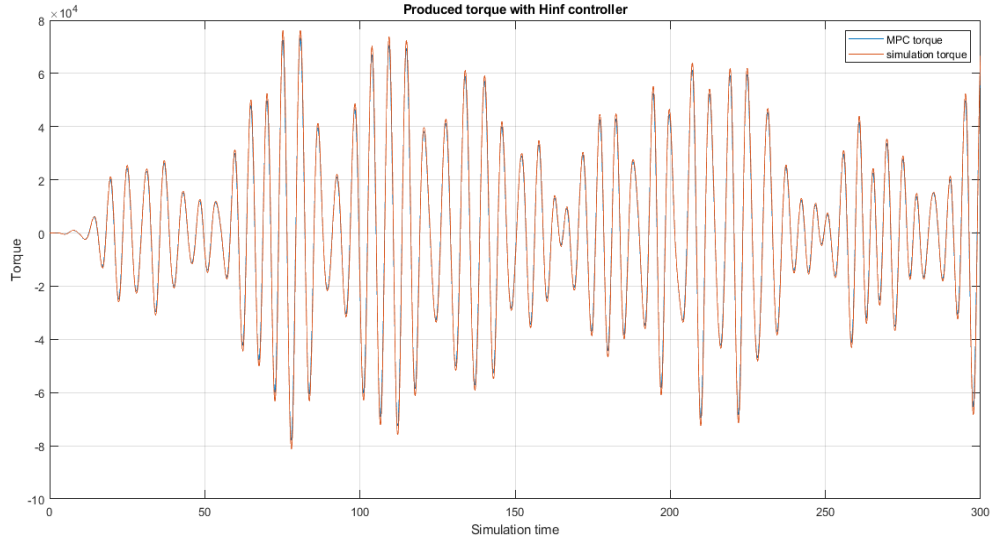


Figure 3.13: *Torque with low order controller.*

The comparison between the MPC power and the Robust one is the following:

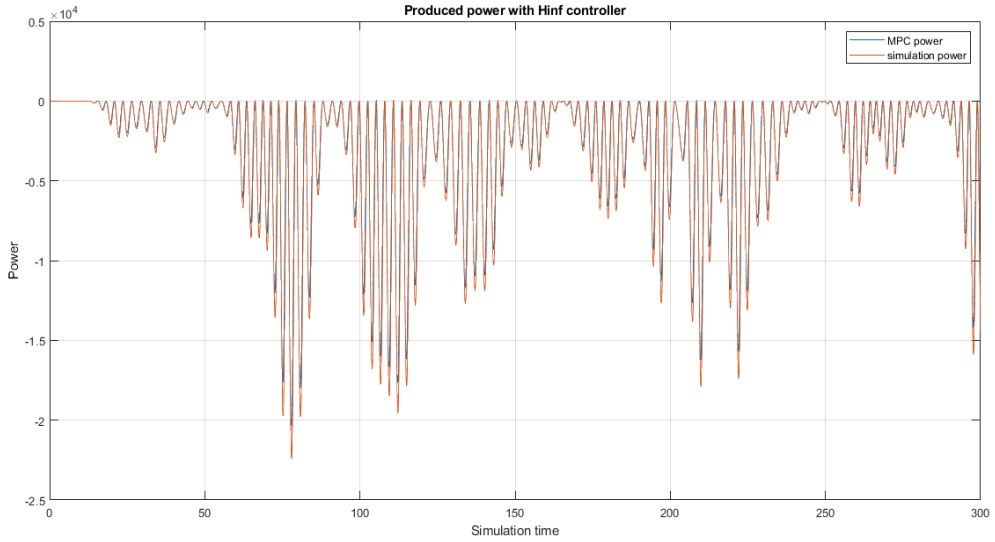


Figure 3.14: *Power with low order controller.*

The results show that the  $H_\infty$  method with the two degree controller provide good performance in terms of tracking and produced power.

The analyses of the Robust stability, nominal performance and Robust performance give, on the other hand, not perfect results:

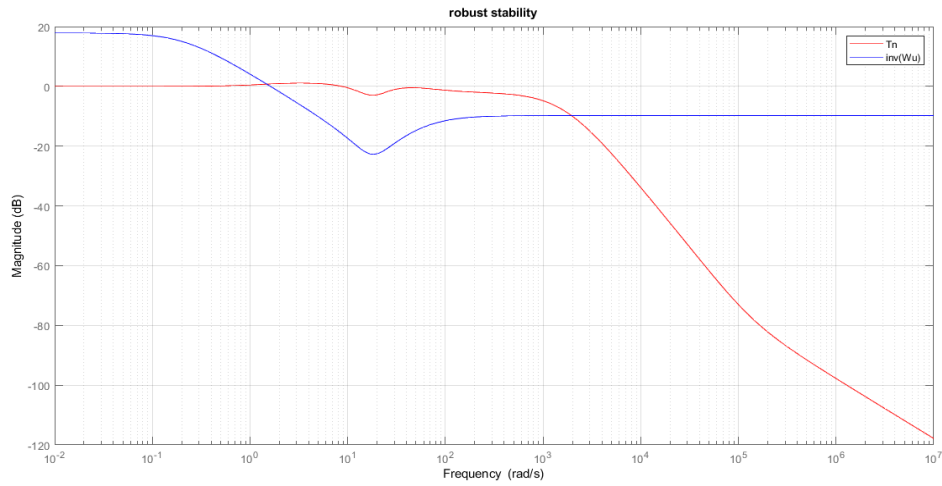


Figure 3.15: *Robust stability condition with low order controller.*

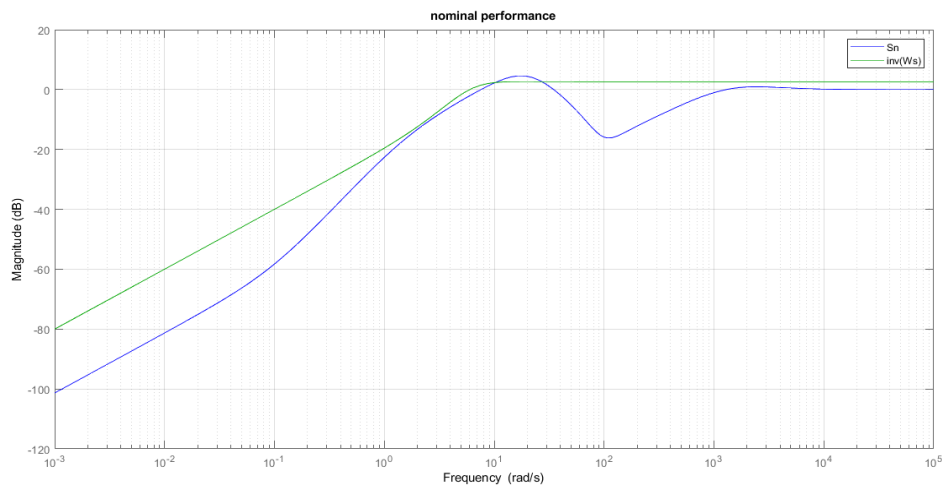


Figure 3.16: *Nominal performance condition with low order controller.*

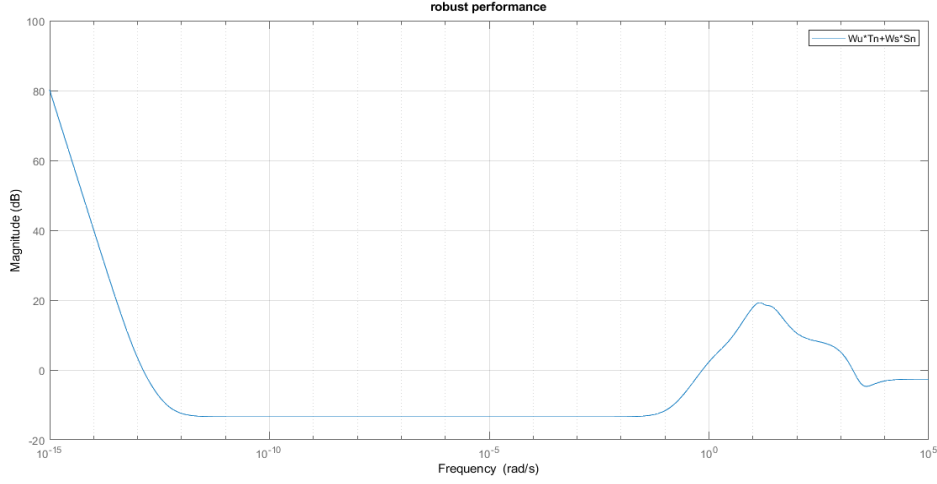


Figure 3.17: Robust performance condition with low order controller.

Despite the not satisfied conditions of Robust stability and Robust performance considering unstructured uncertainty, the perfect tracking of the angular velocity  $\dot{\epsilon}$  of all the four profiles suggests that the model respects the desired conditions, also in produced power terms, so the found model can be considered robustly stable and respects robust performance conditions.

### 3.2.2 High order model $H_\infty$ approach

As the previous approach, the plant and the disturbance transfer function of nine degree found in the SM chapter are taken in analysis. Also for nine degree design, the same time requirements are considered. Considering multiplicative uncertainty

Time requirements	Performance constraints
$K_d = 1$	$G_f = 1$
$ e_r^\infty  < 0.03$	$\rho =  \frac{1}{1+L(jw_0)}  =  S(jw_0) $
$\hat{s} < 0.1$	$\zeta \geq 0.59, T_{po} = 1.05, S_{po} = 1.3$
$t_{s,5\%} < 25s$	$\omega_c \geq 0.18 \frac{rad}{s}$
$t_r < 3s$	$\omega_c \geq 0.23 \frac{rad}{s}$

Table 3.1: Time requirements

and the second plant(4th wave profile) as nominal one, the uncertainty weighted funtion  $W_u$  is:

$$W_u(s) = \frac{1.1519(s + 0.1961)(s^2 + 35.04s + 472.2)(s^2 + 5.665s + 1057)}{(s + 0.1216)(s^2 + 20.59s + 513.4)(s^2 + 3.184s + 948.7)} \quad (3.27)$$

The considered sensitivity function and complementary sensitivity function are the same of two degree design:

$$W_S^{-1}(s) = \frac{0.1s(1 + \frac{s}{3})}{1 + 5.19s + (\frac{s}{3.67})^2}; \quad W_T^{-1}(s) = \frac{1.05}{1 + (\frac{s}{500})^2} \quad (3.28)$$

In order to proceed to the  $H_\infty$  solution, the  $T_{wz}$  must be defined.

$$T_{wz}(s) = \begin{bmatrix} W_1 S_n \\ W_2 T_n \end{bmatrix}$$

$$W_1(s) = W_S(s) \quad , \quad |W_2(jw)| = \max(|W_u(jw)|, |W_T(jw)|)$$

To find  $W_2$ , the two Bode diagrams of  $W_T$  and  $W_u$  are analyzed:

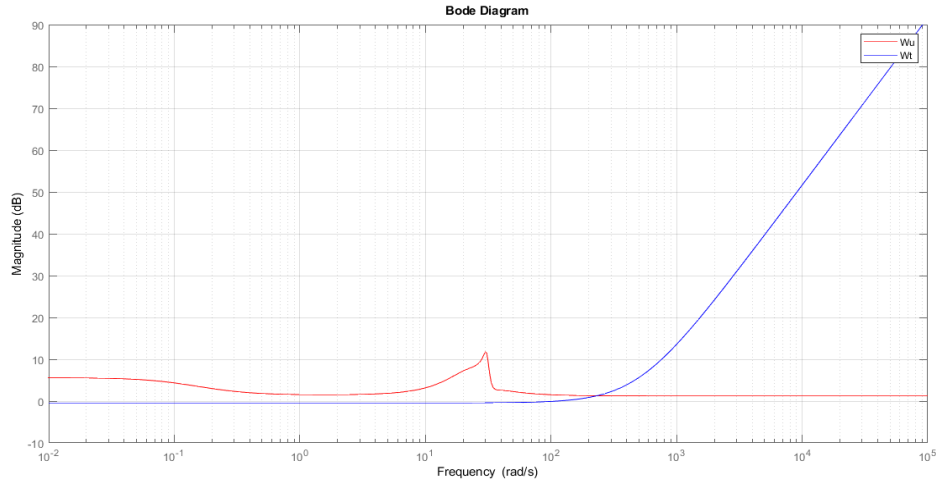


Figure 3.18: Bode diagram of  $W_T$  and  $W_u$ .

As the second degree case, the two functions have a superposition, so it is chosen  $W_2 = W_T$ . Substituting the  $W_1$  pole in origin with a pole in  $0.01w_c$  and doing some gain modifications also on  $W_2$ , the controller is obtained through *lmi optimization*. The first analysis to do is the tracking of the reference, and the correct production of power.

The tracking of reference is the following:

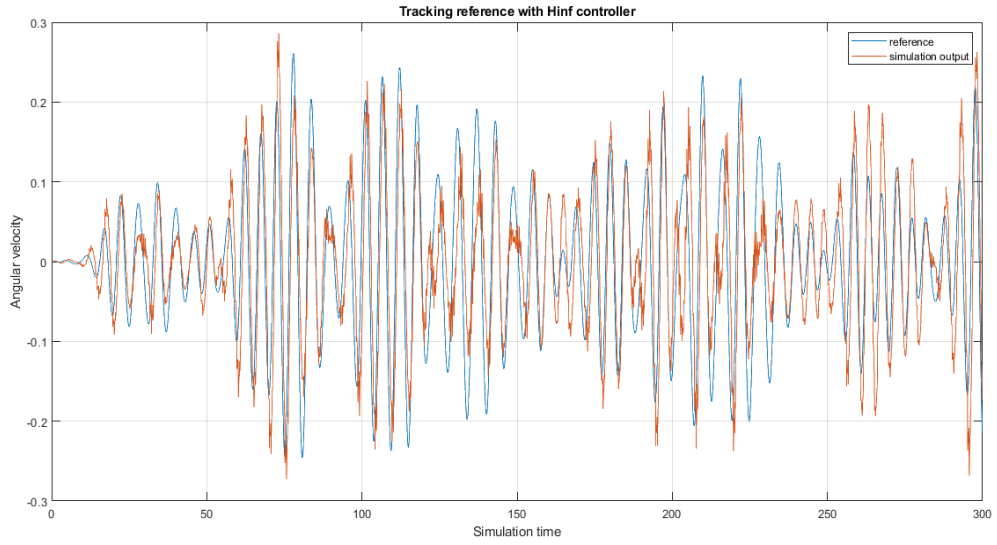


Figure 3.19: *Tracking of the reference with high order controller(case 1).*

The simulation output doesn't follow the reference in a proper way, having an important oscillation of the reference. The comparison between the MPC torque and the Robust one is the following:

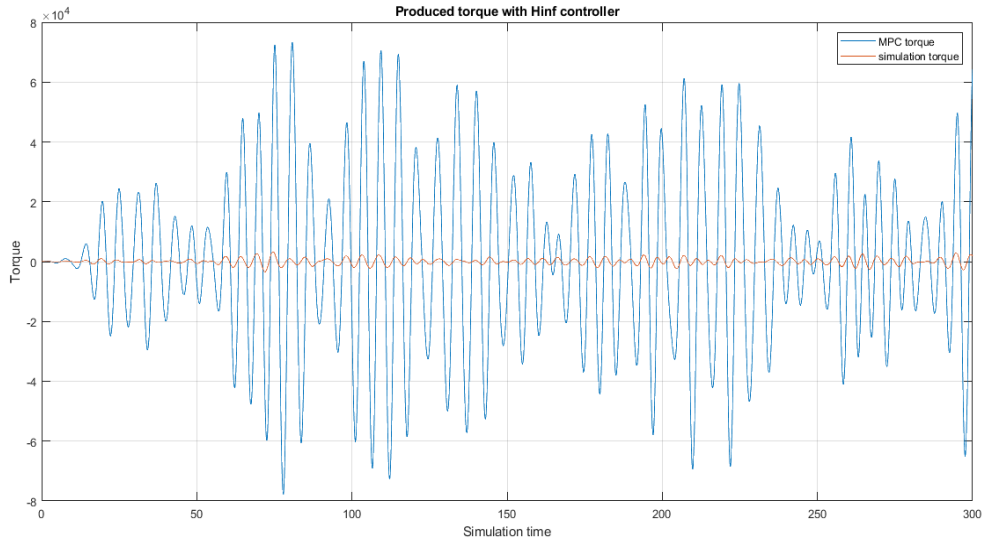


Figure 3.20: *Torque with high order controller(case 1).*

The comparison between the MPC power and the Robust one is the following:

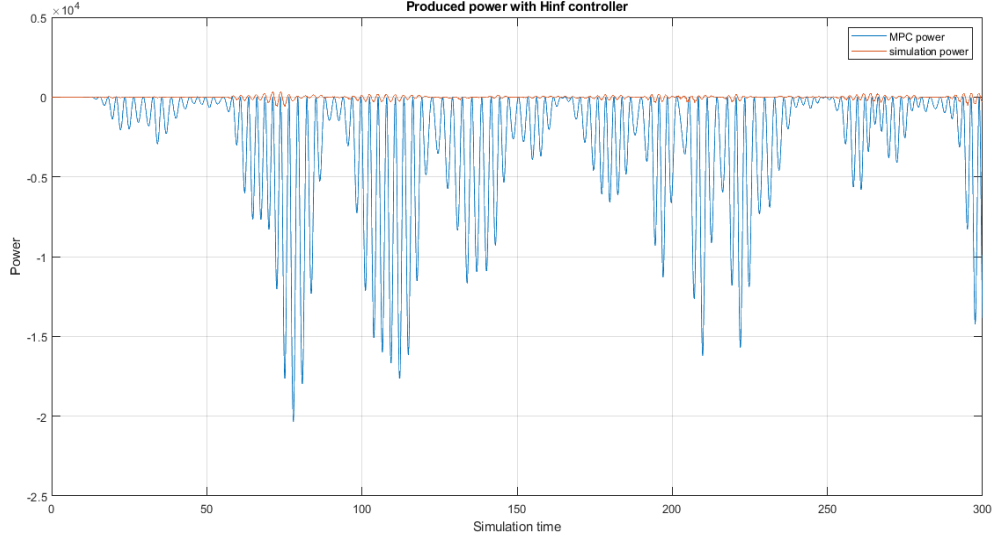


Figure 3.21: *Power with high order controller(case 1).*

The results show that the  $H_\infty$  method with the nine degree controller, using the same  $W_S$  and  $W_T$  of the two degree case, doesn't provide good results in terms of tracking reference, but especially in terms of produced torque and power.

Trying to change the nominal plant, the sensitivity function, the complementary sensitivity function and the uncertainty weighted function, the results are different. Consider as nominal plant the first one(third wave profile).

The respective weighted function  $W_u$  is the following:

$$W_u(s) = \frac{8.5392(s + 85.24)(s^2 + 0.7871s + 0.2172)(s^2 + 4.716s + 64.8)}{(s + 93.92)(s^2 + 1.214s + 0.7142)(s^2 + 3.057s + 25.85)} \quad (3.29)$$

Let's consider the following masks:

$$W_S^{-1}(s) = \frac{0.1s(1 + \frac{s}{0.2})}{1 + 3.8484s + (\frac{s}{0.3674})^2}; \quad W_T^{-1}(s) = \frac{1.05}{1 + (\frac{s}{70})^2} \quad (3.30)$$

$$W_1 = W_S; \quad W_2 = W_T;$$

Substituting in  $W_1$  the pole in origin with another in  $0.01w_c$ , the *lmi optimization* can be done.

The tracking result, the power and the torque production, with the new controller, are the following:

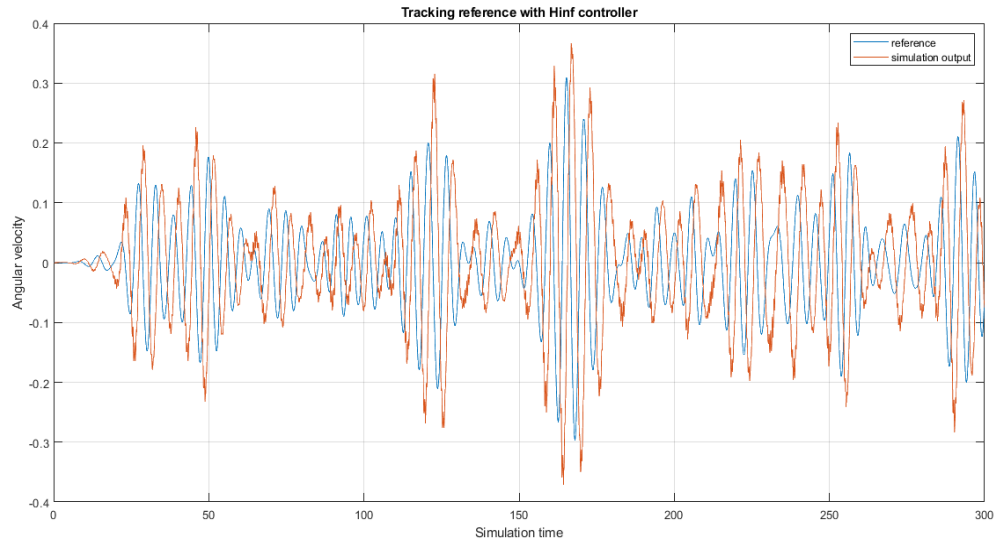


Figure 3.22: *Tracking of the reference with high order controller(case 2).*

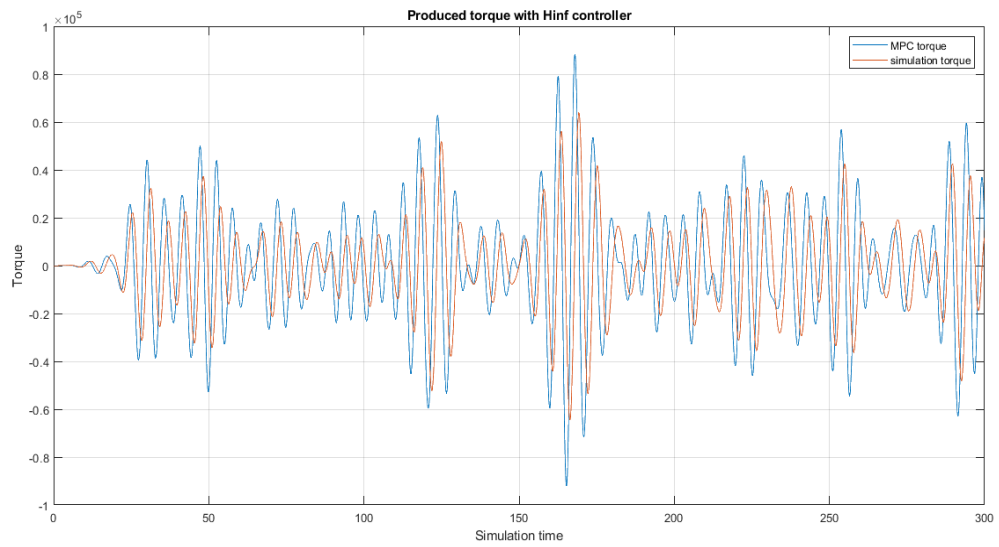


Figure 3.23: *Torque with high order controller(case 2).*

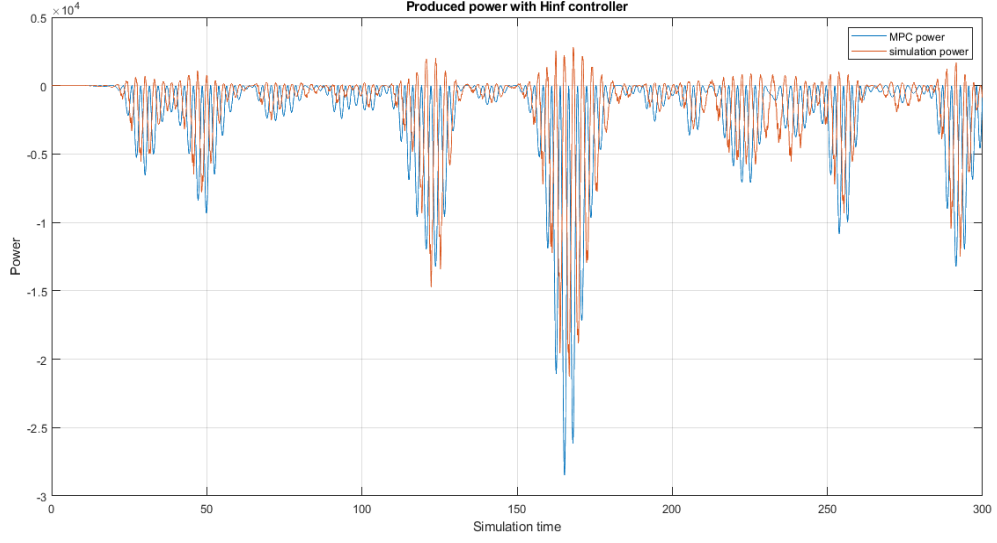


Figure 3.24: *Power with high order controller (case 2).*

As can be seen in the previous figures, the results in this case are few better than the case 1, but on the other hand cannot be considered satisfactory.

It is possible to conclude that despite the Set-Membership Identification has produced optimal results for both two degree and nine degree cases, the  $H_\infty$  approach can provide good results only in low case analyzed. The low order controller reaches an important result in terms of tracking reference and produced power, which are the most important objectives of the thesis work. It is possible now to improve the better controller in the non linear model (MPC Simulink scheme).



## Non linear validation

The second degree controller found in the previous chapter satisfies the tracking reference and the power production objectives. The next step is to validate it in the non linear model: the Simulink model developed with the Model Predictive Control approach is taken in analysis. The final target is to have a controller that, substituted to the controller of the non linear model, gives the same results in terms of angular velocity  $\dot{\epsilon}$ , of torque (output of controller)  $T$  and of power  $P$ .

The final Simulink scheme is the following:

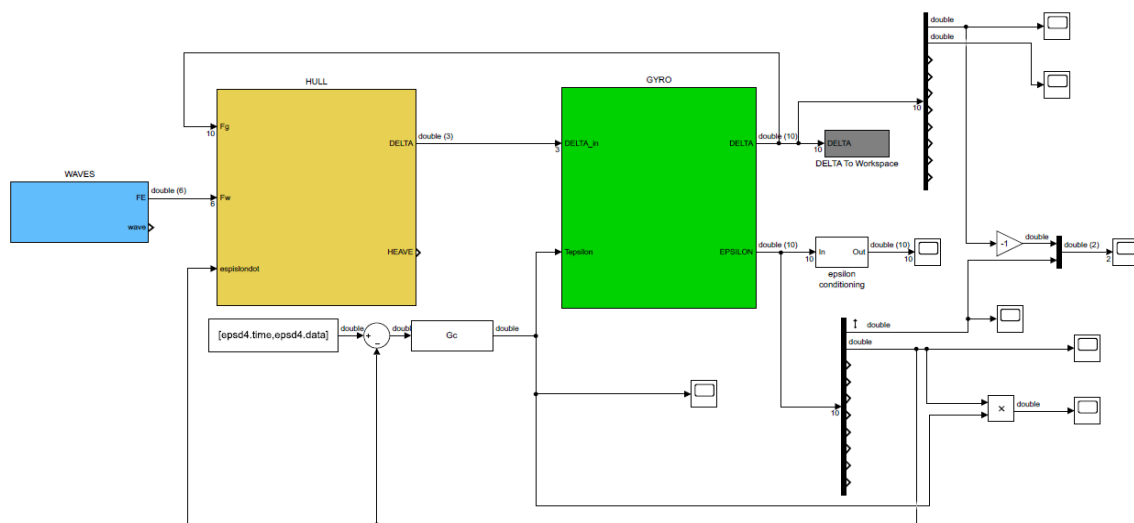


Figure 4.1: *Non linear Simulink model.*

The controller input is the error given from the output of the system subtracted to the angular velocity that is produced, in normal operating conditions, by the MPC Simulink scheme.

Loading the model parameters with the proper Matlab script, the lower order controller and running the model, the results of  $\dot{\epsilon}$  and torque  $T$  are shown in figures 4.2 and 4.3:

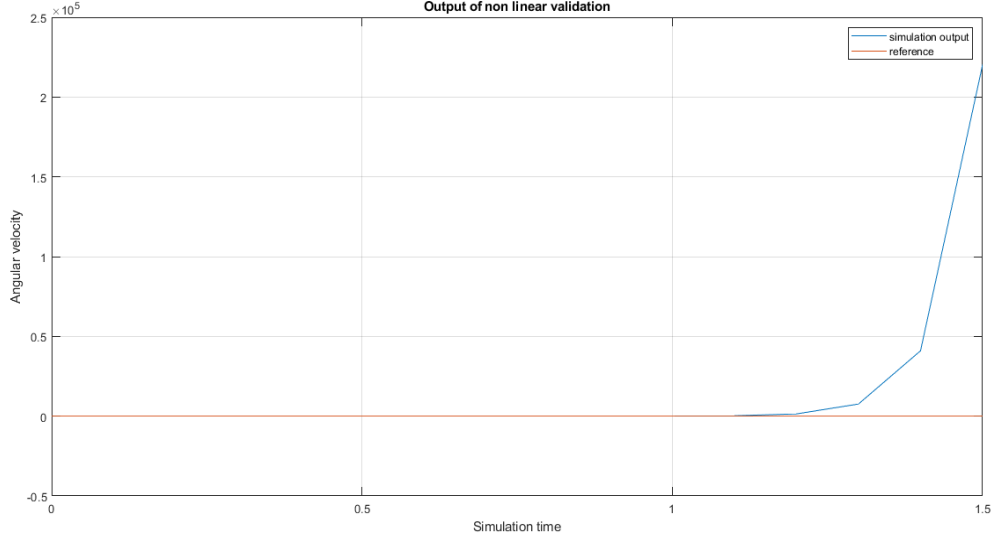


Figure 4.2: *Non linear simulation output.*

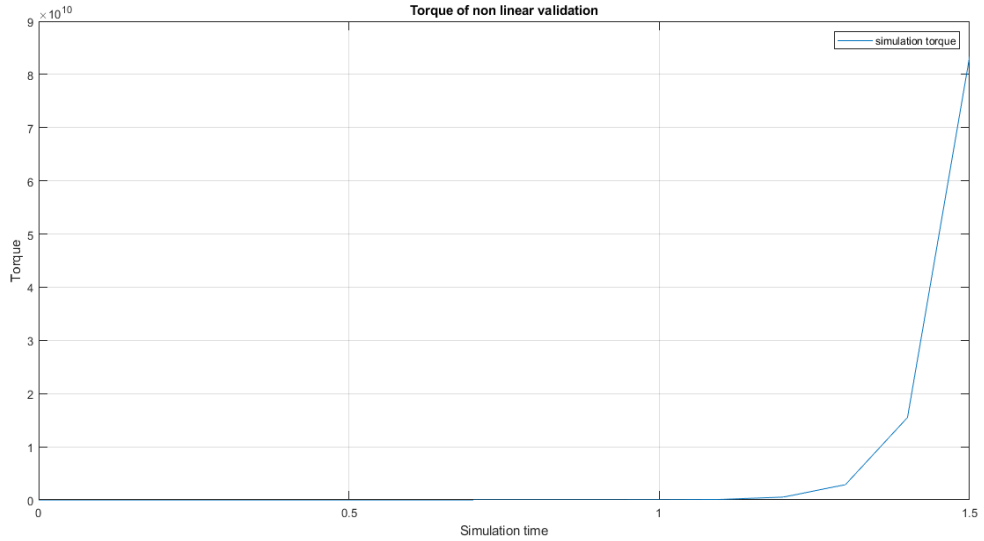
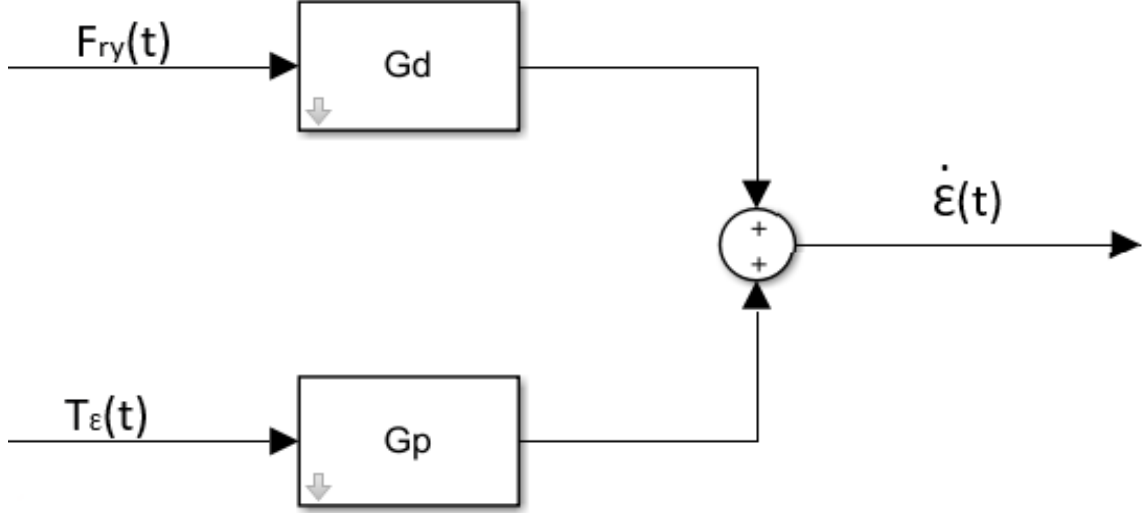
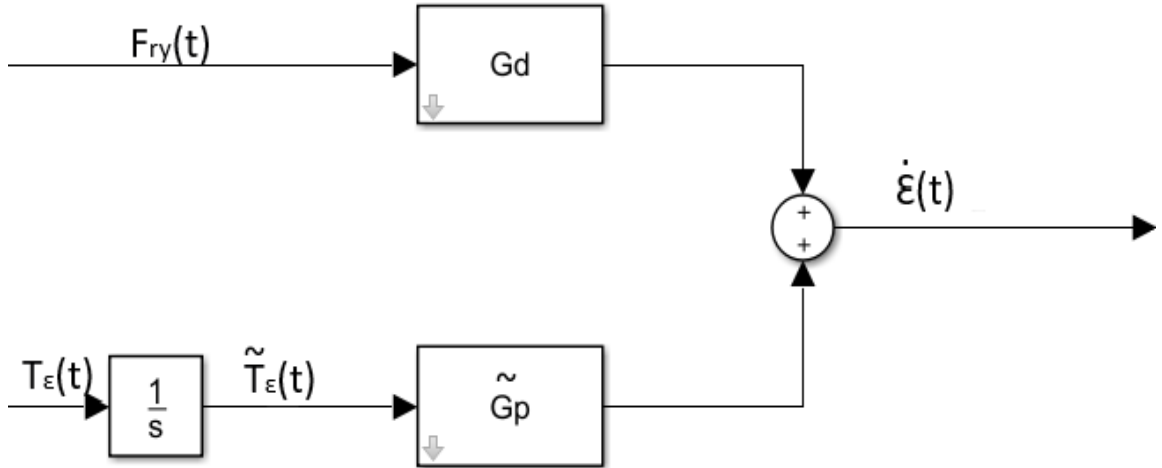


Figure 4.3: *Non linear simulation torque.*

The previous figures show that the output doesn't follow the expected behaviour, but it is divergent, as the torque. It is possible to deduce that despite the Set-Membership produced a good plant with an apparent same behaviour to the non linear model and the  $H_\infty$  produced good results in terms of reference tracking, the

total result cannot be applied in the non linear model. A cause can be an instability of the system with the wrong controller, due to a wrong plant found in SM. In order to solve the problem, a new Set-Membership identification is considered: assuming that the real plant of MPC has a pole in origin, is taken as new dataset the torque multiplied by an integrator  $\frac{1}{s}$ , the angular velocity  $\dot{\epsilon}$  and the input wave force  $F_{ry}$ .


 Figure 4.4: *Original model.*

 Figure 4.5: *New concept model.*

The scheme taken in analysis is the 4.5, where the torque considered is  $\tilde{T}_{\epsilon}$ .

Considering as error structure the output error as in figure 2.8, the new plant transfer function and the new disturbance transfer function, of second degree are:

$$\tilde{G}_p(q^{-1}) = \frac{\dot{\varepsilon}_1(t)}{\tilde{T}_\varepsilon(t)} = \frac{\beta_{10} + \beta_{11}q^{-1} + \beta_{12}q^{-2}}{1 + \alpha_{11}q^{-1} + \alpha_{12}q^{-2}} \quad (4.1)$$

$$G_d(q^{-1}) = \frac{\dot{\varepsilon}_2(t)}{F_{ry}(t)} = \frac{\beta_{20} + \beta_{21}q^{-1} + \beta_{22}q^{-2}}{1 + \alpha_{21}q^{-1} + \alpha_{22}q^{-2}} \quad (4.2)$$

From the 4.1 and 4.2 it is possible to define the equality constraints of the problem:

$$\begin{aligned} \dot{\varepsilon}_1(t)(1 + \alpha_{11}q^{-1} + \alpha_{12}q^{-2}) &= \tilde{T}_\varepsilon(t)(\beta_{10} + \beta_{11}q^{-1} + \beta_{12}q^{-2}) \\ \dot{\varepsilon}_1(t) + \alpha_{11}\dot{\varepsilon}_1(t-1) + \alpha_{12}\dot{\varepsilon}_1(t-2) &= \beta_{10}\tilde{T}_\varepsilon(t) + \beta_{11}\tilde{T}_\varepsilon(t-1) + \beta_{12}\tilde{T}_\varepsilon(t-2) \\ \dot{\varepsilon}_1(t) + \alpha_{11}\dot{\varepsilon}_1(t-1) + \alpha_{12}\dot{\varepsilon}_1(t-2) - \beta_{10}\tilde{T}_\varepsilon(t) - \beta_{11}\tilde{T}_\varepsilon(t-1) - \beta_{12}\tilde{T}_\varepsilon(t-2) &= 0 \end{aligned} \quad (4.3)$$

$$\begin{aligned} \dot{\varepsilon}_2(t)(1 + \alpha_{21}q^{-1} + \alpha_{22}q^{-2}) &= F_{ry}(t)(\beta_{20} + \beta_{21}q^{-1} + \beta_{22}q^{-2}) \\ \dot{\varepsilon}_2(t) + \alpha_{21}\dot{\varepsilon}_2(t-1) + \alpha_{22}\dot{\varepsilon}_2(t-2) &= \beta_{20}F_{ry}(t) + \beta_{21}F_{ry}(t-1) + \beta_{22}F_{ry}(t-2) \\ \dot{\varepsilon}_2(t) + \alpha_{21}\dot{\varepsilon}_2(t-1) + \alpha_{22}\dot{\varepsilon}_2(t-2) - \beta_{20}F_{ry}(t) - \beta_{21}F_{ry}(t-1) - \beta_{22}F_{ry}(t-2) &= 0 \end{aligned} \quad (4.4)$$

The relation that links 4.3 and 4.4 to the real output(angular speed) is the following:

$$\dot{\varepsilon}(t) = \dot{\varepsilon}_1(t) + \dot{\varepsilon}_2(t) \quad (4.5)$$

The parameters  $\dot{\varepsilon}_1(t)$  and  $\dot{\varepsilon}_2(t)$  are the partial outputs of the two transfer functions, unknown, from which the sum gives the real output(PTO shaft angular speed). Considering the equations 4.3, 4.4, 4.5 and 2.12, it is possible to proceed to the *extended feasible parameter set(EFPS)*:

$$\begin{aligned} D_{\theta, \dot{\varepsilon}_1, \dot{\varepsilon}_2, \Delta\eta} &= \{\theta = [\alpha_{11}, \alpha_{12}, \alpha_{21}, \alpha_{22}, \beta_{10}, \beta_{11}, \beta_{12}, \beta_{20}, \beta_{21}, \beta_{22}] \in \mathbb{R}^{10}, \\ &\quad \dot{\varepsilon}_1 \in \mathbb{R}^N, \dot{\varepsilon}_2 \in \mathbb{R}^N, \Delta\eta \in \mathbb{R}^1 : \\ \dot{\varepsilon}_1(t) + \alpha_{11}\dot{\varepsilon}_1(t-1) + \alpha_{12}\dot{\varepsilon}_1(t-2) - \beta_{10}\tilde{T}_\varepsilon(t) - \beta_{11}\tilde{T}_\varepsilon(t-1) - \beta_{12}\tilde{T}_\varepsilon(t-2) &= 0 \\ \dot{\varepsilon}_2(t) + \alpha_{21}\dot{\varepsilon}_2(t-1) + \alpha_{22}\dot{\varepsilon}_2(t-2) - \beta_{20}F_{ry}(t) - \beta_{21}F_{ry}(t-1) - \beta_{22}F_{ry}(t-2) &= 0 \\ y(t) = \dot{\varepsilon}_1(t) + \dot{\varepsilon}_2(t) + \eta(t) &\rightarrow \eta(t) = y(t) - \dot{\varepsilon}_1(t) - \dot{\varepsilon}_2(t) \\ |\eta(t)| &\leq \Delta\eta \end{aligned} \quad (4.6)$$

$$|\eta(t)| \leq \Delta\eta \quad (4.7)$$

Substituting the equation 4.6 into equation 4.7 and evolving the inequality, the

successive equations are obtained:

$$D_{\theta, \dot{\varepsilon}_1, \dot{\varepsilon}_2, \Delta\eta} = \{\theta = [\alpha_{11}, \alpha_{12}, \alpha_{21}, \alpha_{22}, \beta_{10}, \beta_{11}, \beta_{12}, \beta_{20}, \beta_{21}, \beta_{22}] \in \mathbb{R}^{10}, \\ \dot{\varepsilon}_1 \in \mathbb{R}^N, \dot{\varepsilon}_2 \in \mathbb{R}^N, \Delta\eta \in \mathbb{R}^1 :$$

$$\dot{\varepsilon}_1(t) + \alpha_{11}\dot{\varepsilon}_1(t-1) + \alpha_{12}\dot{\varepsilon}_1(t-2) - \beta_{10}\tilde{T}_\varepsilon(t) - \beta_{11}\tilde{T}_\varepsilon(t-1) - \beta_{12}\tilde{T}_\varepsilon(t-2) = 0 \quad (4.8)$$

$$\dot{\varepsilon}_2(t) + \alpha_{21}\dot{\varepsilon}_2(t-1) + \alpha_{22}\dot{\varepsilon}_2(t-2) - \beta_{20}F_{ry}(t) - \beta_{21}F_{ry}(t-1) - \beta_{22}F_{ry}(t-2) = 0 \quad (4.9)$$

$$y(t) - \dot{\varepsilon}_1(t) - \dot{\varepsilon}_2(t) \leq \Delta\eta \quad \rightarrow \quad \Delta\eta - y(t) + \dot{\varepsilon}_1(t) + \dot{\varepsilon}_2(t) \geq 0, \quad \forall t = 1, \dots, N \quad (4.10)$$

$$-y(t) + \dot{\varepsilon}_1(t) + \dot{\varepsilon}_2(t) \leq \Delta\eta \quad \rightarrow \quad \Delta\eta + y(t) - \dot{\varepsilon}_1(t) - \dot{\varepsilon}_2(t) \geq 0, \quad \forall t = 1, \dots, N \quad (4.11)$$

The previous table shows the two equality constraints (4.8, 4.9) and the two inequality constraints 4.10, 4.11, so it is possible now to proceed to the the SparsePOP execution in order to solve the problem.

In this new optimization, the SparsePOP code used is the same of the low order design in chapter 2, however the objective function is not the error  $\eta$  as the previous cases, but the quadratic norm of the error.

The solutions are:

$$\tilde{G}_p = \frac{4.368 \cdot 10^{-7}s^2 + 1.73 \cdot 10^{-6}s + 4.186 \cdot 10^{-6}}{s^2 + 0.9715s + 2.902} \\ G_d = \frac{7.05 \cdot 10^{-9}s^2 - 1.301 \cdot 10^{-7}s - 6.001 \cdot 10^{-8}}{s^2 + 0.1354s + 1.445} \quad (4.12)$$

Proceeding finding a controller through the H-inf design with lmi optimization, the controller obtained is the following:

$$G_c = \frac{5.2637 \cdot 10^{10}(s + 0.418)(s^2 + 0.9715s + 2.902)}{(s + 9.347 \cdot 10^4)(s + 0.01005)(s^2 + 1.543s + 2.955)} \quad (4.13)$$

Loading the controller in the non linear Simulink scheme (4.1), the obtained results in terms of reference tracking and produced power are the following:

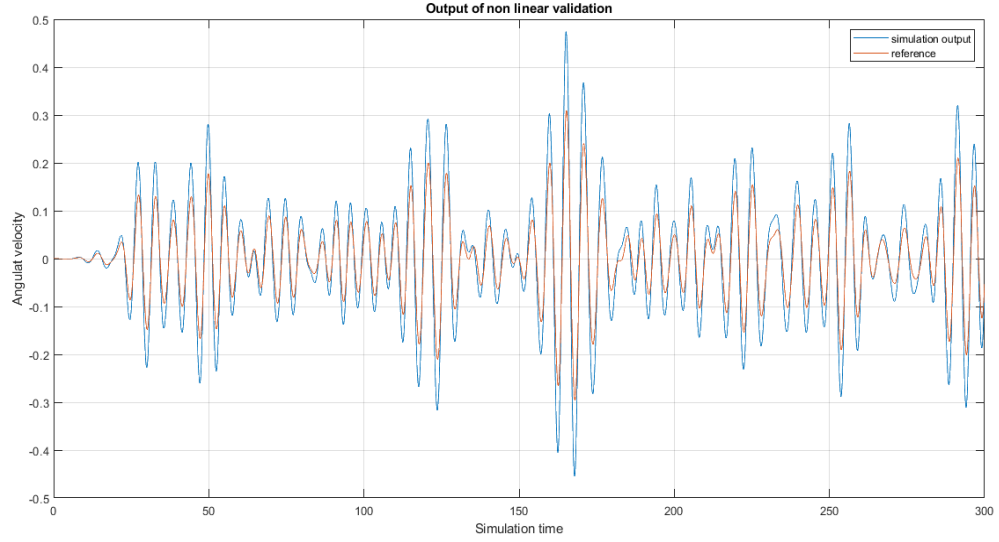


Figure 4.6: *Tracking for wave3.*

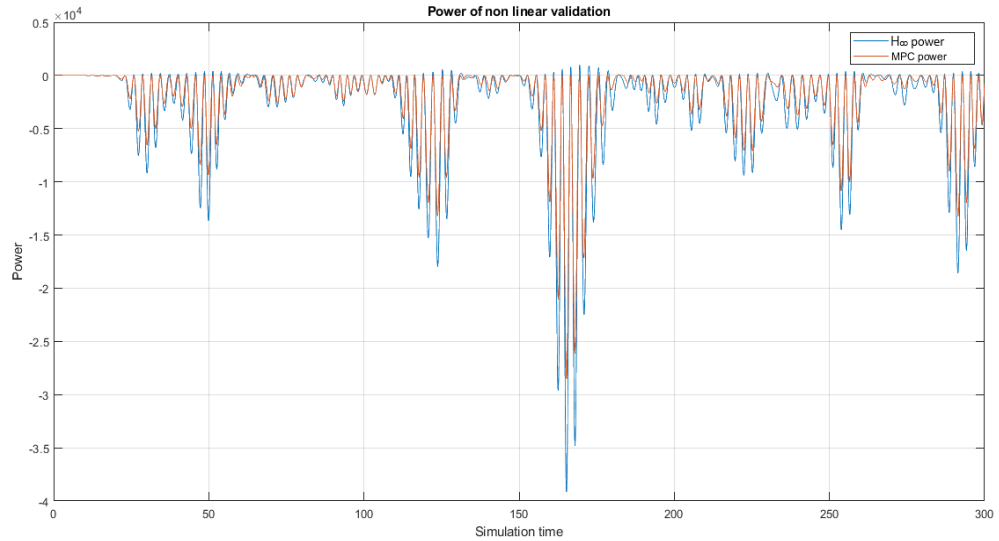


Figure 4.7: *Produced power for wave3.*

As can be seen in the picture 4.6, the simulation output follows in a good way the reference provided by the MPC model, with a bigger gain. The new aspect is that the produced power, as can be seen in figure 4.7, is bigger than the MPC one. Furthermore the same result is obtained for all the 4 wave profiles, obtaining a good tracking and a bigger produced power. This result suggests also a robust stability

and a robust performance of the system, due to the fact that for all the waves the results are optimal.





## Chapter 5

# Conclusions

The thesis work is improved in order to find a good model of the *Iswec system* and a control strategy that can reply the MPC performance in terms of produced power. The Set-Membership approach is used to identify a good plant, using as dataset the output obtained by MPC optimal condition. A second degree identification and a nine degree one have shown optimal results, in terms of reproducing behaviour, in particular the considering angular velocity  $\dot{\epsilon}$  as single output. This highlights that the Set-membership theory is an optimal instrument to identify the plant in this work case and despite the higher complexity in nine degree case, the two degree identification showed the same optimal behaviour with a lower calculation effort.

The chosen control strategy for this purpose is been the Robust Control through  $H_\infty$  approach, using *lmi optimization*. The objective followed is to reproduce the MPC generated power, using the Robust Control theory, that requires a significantly less computational effort. So the problem is oriented to use a reference tracking model, adopting as reference to follow the optimal angular velocity of MPC model, with a robust controller. This approach has shown important results, precisely the tracking and the produced power are very similar to the MPC case with the second degree identified model. This achievement suggests the fact that the system with lower degree is easily usable and controllable, indeed it shows off the best result. In this way, the Robust Control theory is a good candidate to perform a control strategy for the ISWEC system, with better results than PD case, as optimal as the MPC case, but with a lower computational requirement.

Finally the computation shown in the last part of the thesis in the integrator case study highlights optimal results, indeed the obtained controller satisfies also the non linear validation on the generic Simulink model developed for PD and MPC, obtaining an extra produced power bigger than the optimal one obtained with the MPC controller.

The work of the thesis has passed all the previous control strategies developed for the ISWEC system, producing a bigger power, with a low computation requirements. The thesis work opens the road to new studies. The optimal results obtained show that a possible improvement can be the research and the study of an estimator model, that from the wave force predicts the pattern of the angular velocity, used

as reference by the  $H_\infty$  controller. In that way the total model is complete and it will be possible to improve the total result on the real system, in order to test the efficiency and the obtained output.

# Bibliography

- [1] D.MAGAGNA, A.UHLEIN, *Ocean energy development in Europe: Current status and future perspectives*, <https://www-sciencedirect-com.ezproxy.biblio.polito.it/science/article/pii/S2214166915000181>.
- [2] article on *Fact Sheets on the European Union, Renewable energy*, <https://www.europarl.europa.eu/factsheets/en/sheet/70/renewable-energy>.
- [3] G.BRACCO, E.GIORCELLI, G.MATTIAZZO, *ISWEC: A gyroscopic mechanism for wave power exploitation*, <https://www-sciencedirect-com.ezproxy.biblio.polito.it/science/article/pii/S0094114X11001091>.
- [4] G.BRACCO, A.CAGNINI, E.GIORCELLI, G.MATTIAZZO, D.POGGI, M.RAFFERO, *Experimental validation of the Iswec wave to PTO model*, <https://www-sciencedirect-com.ezproxy.biblio.polito.it/science/article/pii/S002980181630110X>.
- [5] G.VISSIO, G.MATTIAZZO, *ISWEC toward the sea - Development, Optimization and Testing of the Device Control Architecture*, <https://iris.polito.it/handle/11583/2697259#.X7gIrzpKjIU>.
- [6] G.BRACCO, M.CANALE, V.CERONE, *Optimizing energy production of an Inertial Sea Wave Energy Converter via Model Predictive Control*, <https://www-sciencedirect-com.ezproxy.biblio.polito.it/science/article/pii/S0967066120300022>.
- [7] V.CERONE, D.PIGA, D.REGRUTO, *Set-Membership Error-in-Variables Identification Through Convex Relaxation Techniques*, IEEE TRANSACTIONS ON AUTOMATIC CONTROL, Vol.57, No.2, pp.517-522, 2012 <https://ieeexplore-ieee-org.ezproxy.biblio.polito.it/document/6018992>.
- [8] V.CERONE, D.PIGA, D.REGRUTO, *Improved parameters bounds for set-membership EIV problems*, INTERNATIONAL JOURNAL OF ADAPTIVE CONTROL AND SIGNAL PROCESSING, Vol.25, No.3, pp.208-227, 2011 <https://onlinelibrary-wiley-com.ezproxy.biblio.polito.it/doi/full/10.1002/acs.1218>.
- [9] V.CERONE, D.PIGA, D.REGRUTO, *Enforcing stability constraints in set-membership identification of linear dynamic systems*, AUTOMATICA, Vol.47, No.11, pp.2488-2494, 2011 <https://www-sciencedirect-com.ezproxy.biblio.polito.it/science/article/pii/S0005109811004067>.
- [10] HAYATO WAKI, SUNYOUNG KIM, MASAKAZU KOJIMA, MASAKAZU MURAMATSU, HIROSHI SUGIMOTO, *Algorithm 883: SparsePOP—A Sparse*

- Semidefinite Programming Relaxation of Polynomial Optimization Problems*, ACM Transactions on Mathematical Software 2008; 35(2): 15:1-15:13 <https://dl-acm-org.ezproxy.biblio.polito.it/doi/abs/10.1145/1377612.1377619>.
- [11] K. ZHOU, J.C. DOYLE *Essential of Robust control*, Pearson College Div, 1997.
- [12] IAN POSTLETHWAITE, SIGURD SKOGESTAD *Multivariable Feedback Control: Analysis and Design, 2nd edition*, John Wiley and Sons , 2005.